

IEET

International Electrical Engineering Transactions

Vol. 3 No. 1 (4)
January-June, 2017
ISSN 2465-4256



An online publication of the EEAAT
Electrical Engineering Academic Association (Thailand)
www.journal.eaat.or.th



IEET – International Electrical Engineering Transactions

This journal is an online publication of the EEAAT, Electrical Engineering Academic Association (Thailand). IEET is published twice a year, ie., the first issue is for January – June and the second issue is for July – December.

EEAAT Journal Committee

Athikom Roeksabutr (Chairman)
Apirat Siritaratiwat
Kosin Chamnongthai
Prayoot Akkaraekthalin

IEET Editor

Somchai Hiranvarodom
Boonyang Plangklang

IEET (International Electrical Engineering Transactions) is published twice a year. Original contributions covering work in all aspects of electrical science, technology, engineering, and applications will be peer-reviewed by experts before publication. Topics of interest include the following: electrical power, electronics, telecommunication, control and system, sensor and measurement, optical technology, computer, information and communication technology (ICT), signal processing, social network tools and applications (apps), engineering education and other related fields.

For online submission of all manuscripts, correspondences, and letters, please visit
www.journal.eeaat.or.th

IEET Editorial Office

EEAAT - Electrical Engineering Academic Association (Thailand)
Room 409, F-Building, 140 Cheum-Sampan Rd.
Nong Chok, Bangkok, Thailand 10530
Tel: +662-988-3655 ext 2216 Fax: +662-988-4026

IEET - International Electrical Engineering Transactions

Volume 3

Number 1 (4)

January – June 2017

PAPERS

Signal Flow Graph Synthesis of General n^{th} -order Voltage Transfer Functions Using Voltage Differencing Buffered Amplifiers (VDBAs)	Worapong Tangsirat Wanlop Surakamponorn	1
Understand True Lightning Protection Neutralize The Environmental Climate	Witsarut Assawachatsakul Krischonme Bhumkittipich Chatchom Sucharitsopit	8
Enhancing Power Electronics and Grid Converter Laboratory Based on Embedded System	C. Tarasantisuk E. Anusurain T. Suyata	12
INFECTION RENAL DIALYSIS DETECTIVE MEDICAL DEVICES FROM IDEA TO END USERS	KESORN PECHRACH WEAVER	17
Fault Characteristics of PV Power Plant Grid Integration by PSCAD/EMTDC	Nattapan Thanomsat Boonyang Plangklang	21
A Methodology for Forecasting Electrical Energy Demand	N. Phuangpompitak B. Prasartkaew	24

Signal Flow Graph Synthesis of General n^{th} -order Voltage Transfer Functions Using Voltage Differencing Buffered Amplifiers (VDBAs)

Worapong Tangsrirat

Faculty of Engineering, King Mongkut's Institute of Technology Ladkrabang (KMITL), Chalongkrung road, Ladkrabang, Bangkok 10520, Thailand
worapong.ta@kmitl.ac.th

Wanlop Surakamponorn

Faculty of Engineering, Rajamangala University of Technology Rattanakosin (RMUTR), Nakhon Pathom 73170, Thailand
wanlop.ltpw@gmail.com

Abstract—This article presents the synthesis procedure of using the signal flow graph (SFG) technique to realize general n^{th} -order voltage transfer function employing voltage differencing buffered amplifiers (VDBAs) as active elements and only capacitors as passive elements. It has been demonstrated that the proposed methodology employs only n VDBAs and n capacitors for the realization of any n^{th} -order voltage transfer function. As illustrative examples, the allpass and the allpole functions as well as standard universal biquadratic filtering realization are designed and simulated. Simulation results by PSPICE have also been provided, which verify the usefulness of the presented design technique.

Keywords— Signal Flow Graph (SFG); Voltage Differencing Buffered Amplifier (VDBA); allpass section; biquadratic filter; allpole lowpass section; voltage-mode circuit

I. INTRODUCTION

It is the well-known fact that the active building blocks are very important in the synthesis of analog signal processing/signal generation circuit solutions. New circuit ideas of active building blocks for providing the potentiality in a class of analog signal processing applications are developed and invented continuously [1]. Among these, the newly introduced active element called voltage differencing buffered amplifier (VDBA) is described [2]-[3], as an alternative to the existing current differencing buffered amplifier (CDBA) [4]. In VDBA, the differential input voltage, rather than current as in CDBA, is transformed to the output current at the z-terminal by the transconductance gain and the voltage drop at the terminal z is then conveyed to the voltages at the terminals w+ and w-. Accordingly, a number of active networks for analog signal processing based on VDBAs have recently been reported [2]-[3], [5]-[8].

In addition, the works given in [4], [9]-[19] have proposed the actively circuit realizations of an n^{th} -order voltage transfer function synthesis based on the signal-flow-graph (SFG) approach employing various active elements. In [4], [9]-[12], the SFG synthesis method for realizing the general n^{th} -order allpole lowpass voltage transfer functions can be obtained. The interesting circuit realizations of an n^{th} -order allpass function synthesis can also be found in [13]-[18]. However, all the

previously mentioned SFG circuit realizations require excessive number of active and passive elements, at least n active devices, n capacitors and n resistors. Although the recent work in [19] has demonstrated the success of a versatile SFG realization of a general n^{th} -order voltage transfer function by using CDBAs, the resulting configuration still employs $n+1$ CDBAs, n capacitors and $2n+4$ resistors.

The purpose of this article is to present a generalized approach based on SFG design method for synthesizing n^{th} -order voltage transfer function with only VDBAs and capacitors. The proposed method is based on drawing a SFG directly from the given transfer function and then obtaining, from the graph, the active-C circuit configurations involving VDBAs. For n^{th} -order transfer function realization, the resulting configuration uses only n VDBAs and n capacitors, which uses less active and passive elements with respect to the previous ones [4], [9]-[19]. It has been shown that the design procedure proposed here is simple and a canonical number of active and passive elements. Design examples and simulation results obtained from PSPICE program illustrate the feasibility of the proposed design procedure.

II. CIRCUIT PRINCIPLE OF VOLTAGE DIFFERENCING BUFFERED AMPLIFIER (VDBA)

Fig.1 shows the circuit symbol and equivalent circuit of the VDBA, in which its conception is based on the use of the transconductance amplifier as an input stage and the voltage follower as an output stage. From Fig.1, the VDBA device has high-impedance voltage differencing input terminals labeled as p and n, high-impedance current output terminal z, and low-impedance outputs of voltage buffer/inverter noted as w+ and w-. The corresponding circuit property can be expressed by the following matrix [1]-[3]:

$$\begin{bmatrix} i_p \\ i_n \\ i_z \\ v_{w+} \\ v_{w-} \end{bmatrix} = \begin{bmatrix} 0 & 0 & 0 & 0 & 0 \\ 0 & 0 & 0 & 0 & 0 \\ g_m & -g_m & 0 & 0 & 0 \\ 0 & 0 & 1 & 0 & 0 \\ 0 & 0 & -1 & 0 & 0 \end{bmatrix} \begin{bmatrix} v_p \\ v_n \\ v_z \\ i_{w+} \\ i_{w-} \end{bmatrix} \quad (1)$$

where g_m is the transconductance gain of the VDBA. According to (1), the differential input voltage between the terminals p and n ($v_p - v_n$) is then converted to a current at the z-terminal (i_z) by a g_m -parameter. The output voltages of terminals w+ (v_{w+}) and w- (v_{w-}) follow the voltage across the z-terminal (v_z). The voltages v_{w+} and v_{w-} will be of equal magnitude but different phases.

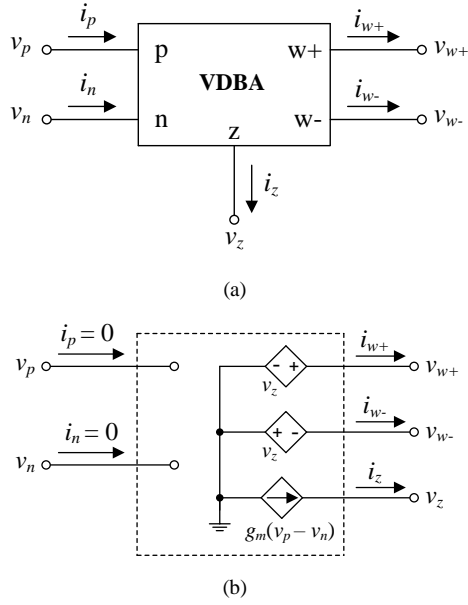


Fig. 1. VDBA (a) circuit symbol (b) equivalent circuit.

III. SFG-BASED SYNTHESIS PROCEDURE

In general, the output voltage of an n^{th} -order transfer function can be characterized by the following expression :

$$V_{out}(s) = \frac{b_n s^n V_n \pm b_{n-1} s^{n-1} V_{n-1} \pm \dots \pm b_2 s^2 V_2 \pm b_1 s V_1 \pm b_0 V_0}{b_n s^n + b_{n-1} s^{n-1} + \dots + b_2 s^2 + b_1 s + b_0} \quad (2)$$

where V_{out} and V_i ($i = 1, 2, \dots, n$) are the output and the input voltages, respectively. The above equation can be represented by the SFG of Fig.2. This graph can be easily verified by using the well-known Mason gain formula [20].

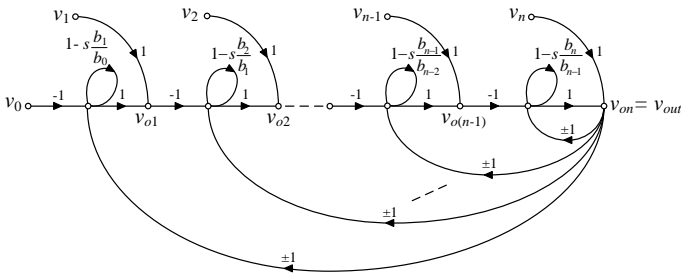


Fig. 2. SFG representation of (2).

It can be observed from Fig.2 that the graph is mainly composed of the cascading connection of the sub-graph as shown in Fig.3(a). Each sub-graph performs the lossless integrator, and its corresponding active-C sub-circuit involving VDBA is shown in Fig.3(b). Therefore, based on Figs.2 and 3, the resulting VDBA-based circuit of (2) can be realized as shown in Fig.4. It is important to note that the proposed technique requires only n VDBAs and n capacitors for realizing any n^{th} -order transfer function.

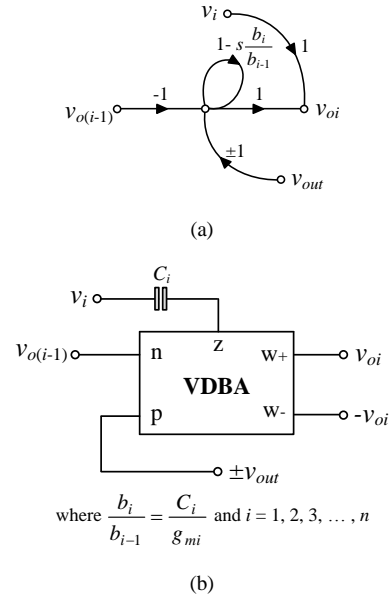


Fig. 3. Sub-graph of Fig. 2 and its corresponding VDBA-based circuit.

By comparing Fig.4 with Fig.2, the design equations in term of circuit component values can be derived as follows :

$$b_0 = 1$$

$$\frac{b_1}{b_0} = \frac{C_1}{g_{m1}}$$

$$\frac{b_2}{b_1} = \frac{C_2}{g_{m2}}$$

⋮

$$\frac{b_{n-1}}{b_{n-2}} = \frac{C_{n-1}}{g_{m(n-1)}}$$

and

$$\frac{b_n}{b_{n-1}} = \frac{C_n}{g_{m(n)}} \quad (3)$$

The above relations imply that the desired coefficient b_i is tunable electronically through adjusting the transconductance g_{mi} of i -th VDBA ($i = 1, 2, \dots, n$).

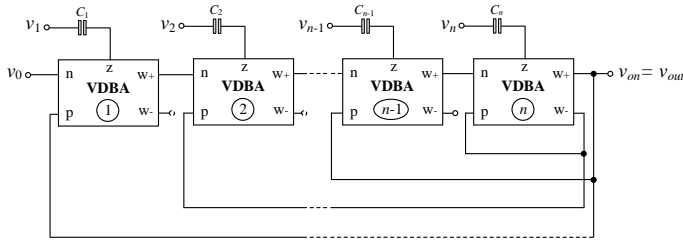


Fig. 4. Resulting VDBA-based circuit realization of a general n^{th} -order voltage transfer function of (2).

IV. DESIGN EXAMPLES

The utility of the proposed design procedure will be demonstrated by the following illustrative examples.

A. Allpass Section Realization

According to (2), let $n = 1$ and $V_{in} = V_0 = V_1$, then the first-order allpass filtering section can be characterized by a transfer function of the following general form.

$$\frac{V_{out}(s)}{V_{in}(s)} = \frac{b_1s - b_0}{b_1s + b_0} \tag{4}$$

In order to represent the SFG of (4), Fig.2 is redrawn as in Fig.5(a), and its corresponding VDBA-C circuit realization can then be modified as Fig.5(b). As can be observed, the realized first-order circuit consists of only one VDBA and one capacitor. Based on the relation of (3), Eq. (4) becomes :

$$\frac{V_{out}(s)}{V_{in}(s)} = \frac{\left(\frac{C_1}{g_{m1}}\right)s - 1}{\left(\frac{C_1}{g_{m1}}\right)s + 1} \tag{5}$$

In this case, the pole frequency (ω_p) and phase shift (ϕ) of the circuit are obtained respectively as:

$$\omega_p = 2\pi f_p = \frac{g_{m1}}{C_1} \tag{6}$$

and
$$\phi = \pi - 2 \tan^{-1}\left(\frac{\omega C_1}{g_{m1}}\right) \tag{7}$$

Similarly, if $n = 3$ and $V_{in} = V_0 = V_1 = V_2$, the third-order allpass filtering section can be realized with the following normalized characteristic function [21].

$$\frac{V_{out}(s)}{V_{in}(s)} = \frac{s^3 - 2s^2 + 2s - 1}{s^3 + 2s^2 + 2s + 1} \tag{8}$$

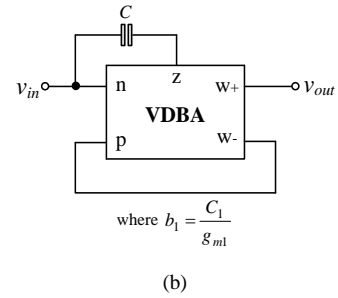
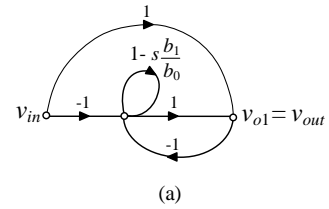


Fig. 5. SFG realization of the 1st-order allpass filter section. (a) SFG representation (b) VDBA-based circuit realization

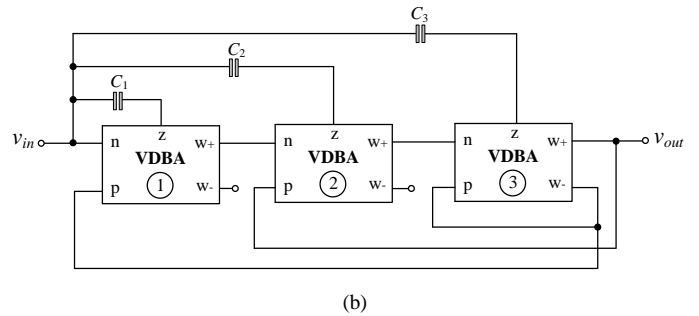
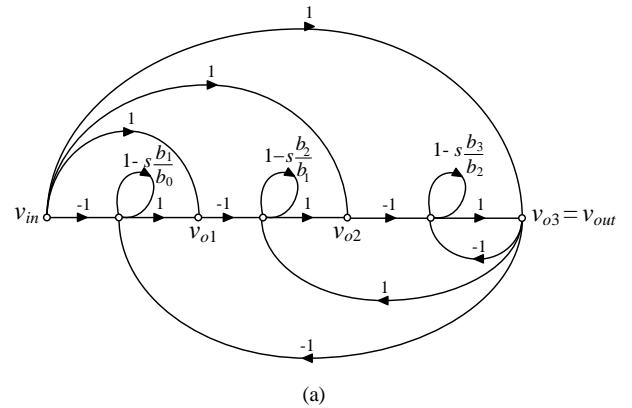


Fig. 6. SFG realization of the 3rd-order allpass filter section. (a) SFG representation (b) VDBA-based circuit realization

The SFG of Fig.6(a) simply represents the above transfer function, and its corresponding circuit realization obtained by using the above procedure can be shown in Fig.6(b). Using (3), the design equations for the circuit of Fig.6(b) are as follows:

$$b_1 = \frac{C_1}{g_{m1}} = 2, \quad \frac{b_2}{b_1} = \frac{C_2}{g_{m2}} = 1 \quad \text{and} \quad \frac{b_3}{b_2} = \frac{C_3}{g_{m3}} = \frac{1}{2} \quad (9)$$

From above relations, the normalized component values are calculated as : $C_1 = C_2 = C_3 = 1$ F, $g_{m1} = 1/2$ A/V, $g_{m2} = 1$ A/V and $g_{m3} = 2$ A/V. Routine circuit analysis of Fig.6(b) yields the following transfer function :

$$\frac{V_{out}(s)}{V_{in}(s)} = \frac{s^3 - \left(\frac{g_{m3}}{C_3}\right)s^2 + \left(\frac{g_{m2}g_{m3}}{C_2C_3}\right)s - \left(\frac{g_{m1}g_{m2}g_{m3}}{C_1C_2C_3}\right)}{s^3 + \left(\frac{g_{m3}}{C_3}\right)s^2 + \left(\frac{g_{m2}g_{m3}}{C_2C_3}\right)s + \left(\frac{g_{m1}g_{m2}g_{m3}}{C_1C_2C_3}\right)} \quad (10)$$

The active and passive sensitivities of ω_p and the quality factor (Q) are calculated using relations given in [22]. The results of active and passive sensitivity analysis of various parameters for the proposed filter are given in Table I. It is clearly seen that all the sensitivities are low and within unity in magnitude.

TABLE I. CIRCUIT SENSITIVITY OF FIG.6(B).

	g_{m1}	g_{m2}	g_{m3}	C_1	C_2	C_3
b_0	1	1	1	-1	-1	-1
b_1	0	1	1	0	-1	-1
b_2	0	0	1	0	0	-1
ω_p	0	1	0	0	-1	0
Q	1	0	-1	-1	0	1

B. Standard Universal Biquadratic Functions

To further illustrate the usefulness of the given design method, the standard universal biquadratic function ($n = 2$) is designed. The standard second-order voltage transfer functions derived from (2) can be given by the following expression:

$$V_{out}(s) = \frac{b_2s^2V_2 - b_1sV_1 + b_0V_0}{b_2s^2 + b_1s + b_0} \quad (11)$$

where its graph and circuit realization can be drawn in Fig.7(a) and 7(b), respectively. In this case, it has been shown that two VDDBAs and two capacitors are required. As a result from (3) and (11), the output voltage function of Fig.7(b) which gives element values can be written as:

$$V_{out}(s) = \frac{s^2V_2 - \left(\frac{g_{m2}}{C_2}\right)sV_1 + \left(\frac{g_{m1}g_{m2}}{C_1C_2}\right)V_0}{s^2 + \left(\frac{g_{m2}}{C_2}\right)s + \left(\frac{g_{m1}g_{m2}}{C_1C_2}\right)} \quad (12)$$

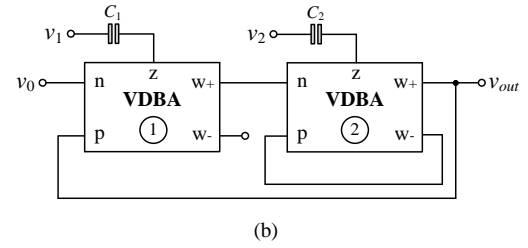
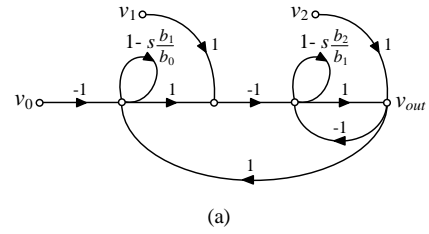


Fig. 7. SFG realization of the standard 2nd-order universal filtering functions. (a) SFG representation (b) VDBA-based circuit realization

Observe that all the standard biquadratic voltage functions can be realized from Fig.7(b) by the following conditions.

- 1) The lowpass (LP) function is obtained, if $V_{in} = V_0$ and $V_2 = V_1 = 0$.
- 2) The highpass (HP) function is obtained, if $V_{in} = V_2$ and $V_1 = V_0 = 0$.
- 3) The bandpass (BP) function is obtained, if $V_{in} = V_1$ and $V_2 = V_0 = 0$.
- 4) The bandstop (BS) function is obtained, if $V_{in} = V_2 = V_0$ and $V_1 = 0$.
- 5) The allpass (AP) function is obtained, if $V_{in} = V_2 = V_1 = V_0$.

Also from (12), the parameters ω_p and Q of all biquadratic functions can be found as, respectively:

$$\omega_p = \sqrt{\frac{g_{m1}g_{m2}}{C_1C_2}} \quad (13)$$

and

$$Q = \sqrt{\frac{g_{m1}C_2}{g_{m2}C_1}} \quad (14)$$

C. Allpole Lowpass Function

Next, the realization of the third-order allpole lowpass transfer function is considered. Generally, the voltage transfer function of the normalized third-order Butterworth lowpass filter is defined as :

$$\frac{V_{out}(s)}{V_{in}(s)} = \frac{1}{b_3s^3 + b_2s^2 + b_1s + b_0} = \frac{1}{s^3 + 2s^2 + 2s + 1} \quad (15)$$

To synthesis the n^{th} -order allpole transfer function, it can be easily realized from the SFG of Fig.2 by setting $v_{in} = v_0$ and removing all the feed-forward parts (v_1, v_2, \dots, v_n). As a consequence, the SFG actualization for $n = 3$ corresponding to (15) is obtained as Fig.8(a), and the realization of its VDBA-C circuit is thus shown in Fig.8(b). Obviously, the relationship among the circuit parameters is the same as (9). Therefore, Eq. (15) turns to :

$$\frac{V_{out}(s)}{V_{in}(s)} = \frac{g_{m1}g_{m2}g_{m3}}{C_1C_2C_3} \frac{1}{s^3 + \left(\frac{g_{m3}}{C_3}\right)s^2 + \left(\frac{g_{m2}g_{m3}}{C_2C_3}\right)s + \left(\frac{g_{m1}g_{m2}g_{m3}}{C_1C_2C_3}\right)} \quad (16)$$

In the same manner, the sensitivity analysis shows that the sensitivities of ω_p and Q with respect to the active and passive components are the same as summarized in Table I.

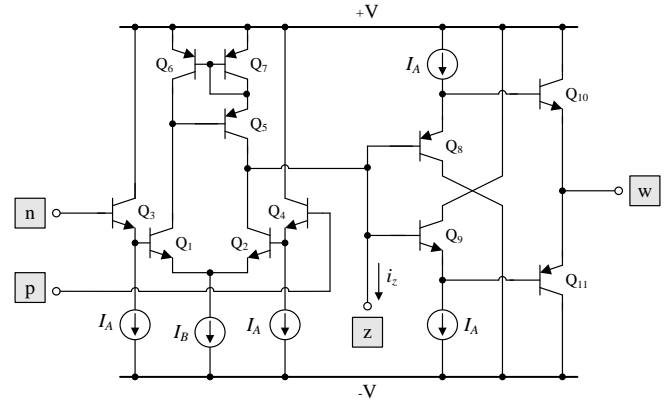


Fig. 9. Bipolar realization of the VDBA used in simulations.

A. Allpass Section

As an illustrative example, the first-order allpass filter section in Fig.5(b) was design to obtain the allpass voltage response with the pole frequency of $f_p \cong 766$ kHz. For this purpose, the following active and passive components were chosen as : $I_{B1} = 50 \mu\text{A}$ ($g_{m1} \cong 0.96$ mA/V) and $C_1 = 0.2$ nF. Fig. 10 shows the ideal and simulated frequency characteristics of the first-order allpass filter realization of Fig. 5(b). The simulated time-domain responses for v_{in} and v_{out} are also shown in Fig.11, where the phase shift is recorded to be 84° .

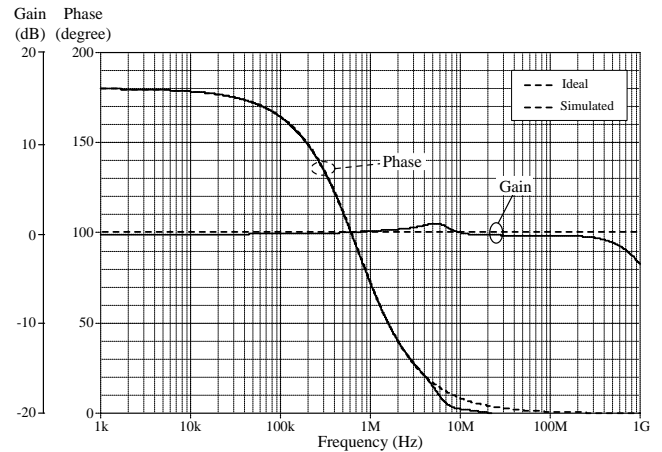


Fig. 10. Ideal and simulated frequency responses of the 1st-order allpass filter in Fig.5(b).

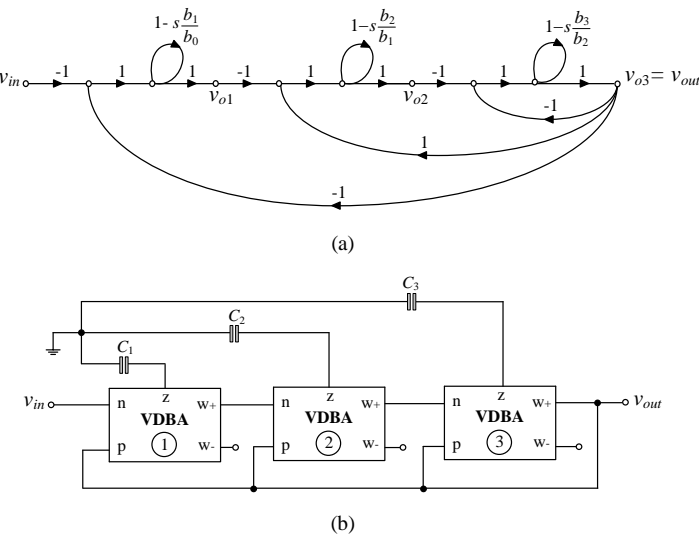


Fig. 8. SFG realization of the 3rd-order allpole lowpass function. (a) SFG representation (b) VDBA-based circuit realization

V. COMPUTER SIMULATION AND PERFORMANCE VERIFICATION

PSPICE simulations have been carried out to verify the feasibility of the designed procedure. In simulations, the bipolar realization of the VDBA circuit shown in Fig.9 [23] has been performed with the bipolar transistor array model PR100N (PNP) and NP100N (NPN) from AT&T. The supply voltages were $+V = -V = 1.5\text{V}$, and biasing currents were $I_A = 50 \mu\text{A}$. In Fig.9, the small-signal effective transconductance gain (g_m) of the VDBA can be given by :

$$g_m = \frac{I_B}{2V_T} \quad (17)$$

where $V_T \cong 26$ mV at 27° C is the thermal voltage, and I_B is the external DC bias current.

To obtain the third-order allpass voltage response with the pole frequency of $f_p \cong 159$ kHz, the circuit of Fig.6(b) was realized with $g_{m1} \cong 0.58$ mA/V ($I_{B1} = 30 \mu\text{A}$), $g_{m2} \cong 1.08$ mA/V ($I_{B2} = 56 \mu\text{A}$), $g_{m3} \cong 2.15$ mA/V ($I_{B3} = 112 \mu\text{A}$) and $C_1 = C_2 = C_3 = 1$ nF. As a result of circuit simulations, input and output sinusoidal waveforms for the circuit of Fig.6(b) are shown in Fig.12. The circuit was inputted with a sinusoidal signal of 20 mV (peak) at a frequency of 159 kHz, and the output voltage with the phase difference of 262° was obtained. The total harmonic distortion (THD) variation of the output voltage for varying input signal amplitude at $f = 159$ kHz was also investigated, and the results are plotted in Fig.13. These

variations are found within 2.4% at the range of input voltage $v_{in} \leq 100$ mV (peak-to-peak).

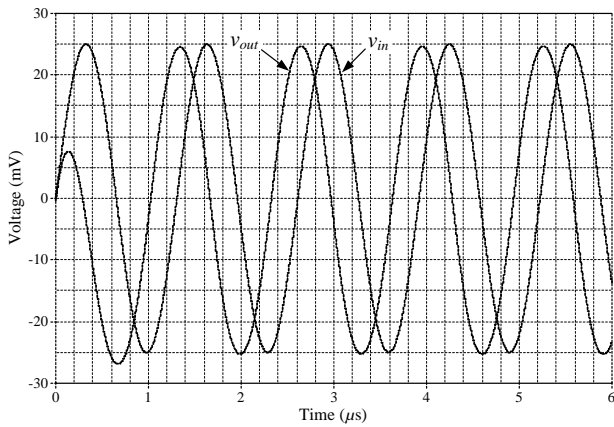


Fig. 11. Simulated input and output transient responses of the 1st-order allpass filter in Fig.5(b).

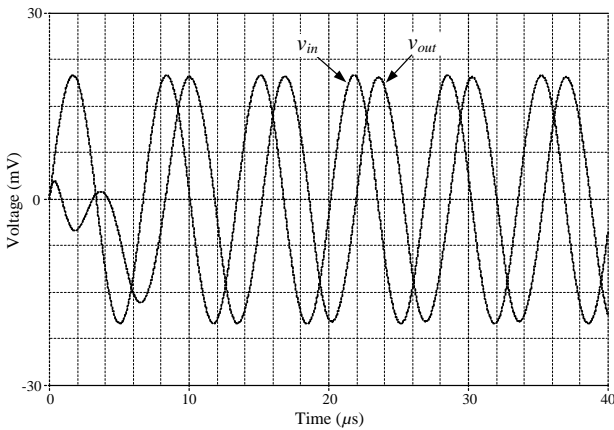


Fig. 12. Simulated input and output transient responses of the 3rd-order allpass filter in Fig.6(b).

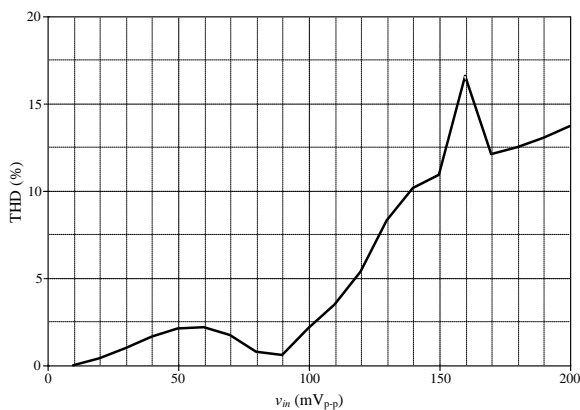


Fig. 13. THD variation of the output voltage with the input signal amplitude at $f = 159$ kHz.

B. Universal Biquadratic Filter

Let us consider the standard universal biquadratic filter as shown in Fig.7(b), with $I_{B1} = I_{B2} = 76 \mu A$ ($g_{m1} = g_{m2} \cong 1.414$

mA/V) and $C_1 = C_2 = 1$ nF. According to (13) and (14), this results in $f_p = 255$ kHz and $Q = 1$. The ideal and simulated frequency responses of the filter are shown on Figs.14 and 15. From the results, the locations of the simulated f_p are about: 215.29 kHz, 219.92 kHz, 217.30 kHz, and 213.98 kHz for LP, HP, BS, and BP responses, which correspond to the following absolute errors: 4.33%, 3.28%, 3.38%, and 4.92%, respectively.

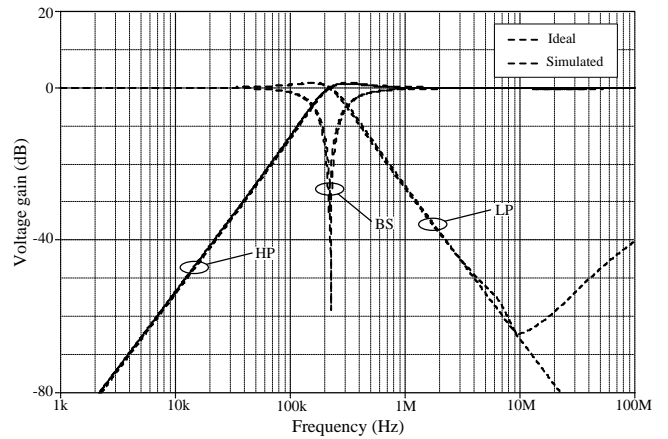


Fig. 14. Simulated frequency characteristics for the LP, HP, and BS responses of Fig.7(b).

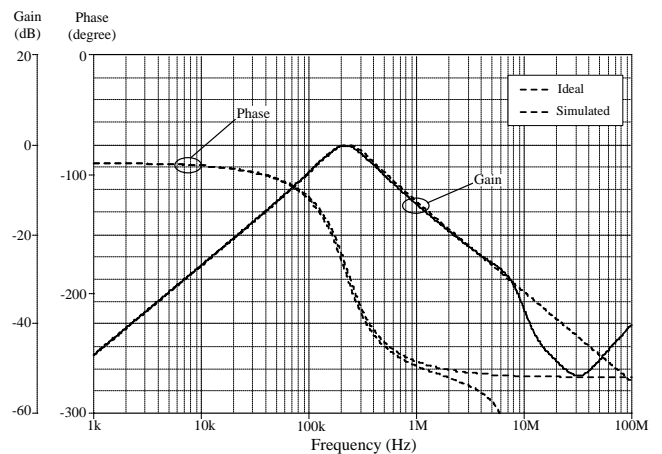


Fig. 15. Simulated BP frequency response of Fig.7(b).

C. Allpole Lowpass Filter

A further interesting feature of the design procedure given above concerns the illustrative third-order allpole lowpass configuration of Fig.8(b). As example, the circuit was designed to realize the lowpass filter response with $\omega_p = 10^6$ rad/sec. In this case, the de-normalized component values were selected as : $C_1 = C_2 = C_3 = 1$ nF, $g_{m1} = 2$ mA/V ($I_{B1} \cong 104 \mu A$), $g_{m2} = 1$ mA/V ($I_{B2} \cong 52 \mu A$), and $g_{m3} = 1/2$ mA/V ($I_{B3} \cong 26 \mu A$). The simulated responses comparing with the theoretical values are shown in Fig.16. From the results, it can be observed that the simulation results agree very well with theoretical predictions.

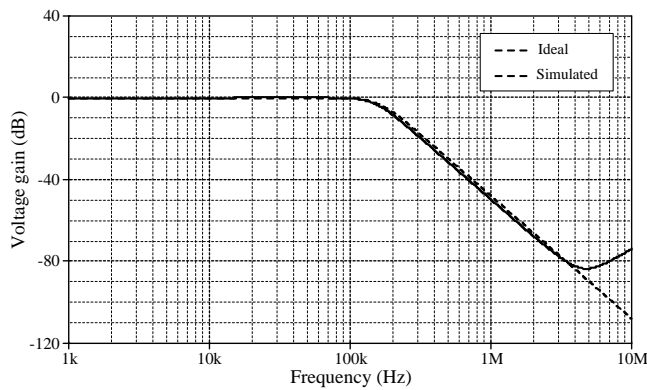


Fig. 16. Ideal and simulated frequency responses of Fig.8(b).

VI. SUMMARY

A simple synthesis procedure is presented for the realization of general n^{th} -order voltage transfer function by a resistor-less (active-C) circuit. The synthesis technique is based on the use of the signal flow graph. For any n^{th} -order system realization, the resulting active circuit needs only n VDAs and n capacitors. The attractive features of the proposed structures realized by this design method are simple structure, canonic in a number of active and passive components and provide the ability of electronic tuning. The simulation results from PSPICE are in excellent agreement with theoretical assumptions.

ACKNOWLEDGMENT

The authors would like to thank Miss Oosana Onjan for performing the computer simulations of this work.

REFERENCES

- [1] D. Biolk, R. Senani, V. Biolkova, and Z. Kolka, "Active elements for analog signal processing : classification, review, and new proposals", *Radioengineering*, vol. 17, no. 4, pp. 15-32, 2008.
- [2] F. Kacar, A. Yesil, A. Noori, "New CMOS realization of voltage differencing buffered amplifier and its biquad filter application", *Radioengineering*, vol. 21, no.1, pp. 333-339, 2012.
- [3] R. Sotner, J. Jerabek, N. Herencsar, "Voltage differencing buffered/inverted amplifiers and their applications for signal generation", *Radioengineering*, vol.22, no.2, pp.490-504, 2013.
- [4] C. Acar and S. Ozoguz, "A new versatile building block : current differencing buffered amplifier suitable for analog signal processing filters", *Microelectronics J.*, vol.30, pp.157-160, 1999.
- [5] N. Khatib and D. Biolk, "New voltage mode universal filter based on promising structure of voltage differencing buffered amplifier," *Proc. RADIOELEKTRONIKA-2013*, Pardubice, Czech Republic, 16-17 April, pp. 177-181, 2013.
- [6] A. Yesil, F. Kacar, and K. Gurkan, "Lossless grounded inductance simulator employing single VDBA and its experimental band-pass filter application," *Int. J. Electron. Commun. (AEU)*, vol. 68, pp. 143-150, 2014.
- [7] S. Unhavanich, O. Onjan and W. Tangsrirat, "Tunable capacitance multiplier with a single voltage differencing buffered amplifier", *Proc. Int. MultiConf. Engineers and Computer Scientists 2016 (IMECS 2016)*, 16-18 March, Hong Kong, pp. 568-571, 2016.
- [8] O. Channumsin and W. Tangsrirat, "Actively synthetic floating inductor using voltage differencing buffered amplifiers", *Proc. Int. MultiConf. Engineers and Computer Scientists 2016 (IMECS 2016)*, 16-18 March, Hong Kong, pp. 620-623, 2016.
- [9] F. Anday, "Active realization of n^{th} -order low-pass transfer functions," *IEEE Trans. Circuits Syst.*, vol. CAS-24, no. 12, pp. 745-746, 1977.
- [10] C. Acar, "Realisation of n^{th} -order lowpass voltage transfer function by active R circuit: signal-flow-graph approach," *Electron. Lett.*, vol. 14, no. 23, pp. 729-730, 1978.
- [11] C. Acar, "Nth-order lowpass voltage transfer function synthesis using CCII+: signal flow graph approach," *Electron. Lett.*, vol. 32, no. 3, pp. 159-160, 1996.
- [12] E. O. Gunes and F. Anday, "CFA based fully integrated n^{th} -order lowpass filter," *Electron. Lett.*, vol. 33, no. 7, pp. 571-573, 1997.
- [13] C. Acar, "Nth-order allpass voltage transfer function synthesis using CCII+s: signal-flow graph approach," *Electron. Lett.*, vol. 32, no. 8, pp. 727-728, 1996.
- [14] E. O. Gunes and F. Anday, "An n^{th} -order allpass voltage transfer function synthesis using commercially available active components," *Microelectron. J.*, vol. 30, pp. 895-898, 1999.
- [15] C. Acar, "Nth-order voltage transfer function synthesis using commercially available active component: signal-flow graph," *Electron. Lett.*, vol. 32, no. 21, pp. 1933-1934, 1996.
- [16] E. O. Gunes and F. Anday, "Realisation of n^{th} -order voltage transfer function using CCII+," *Electron. Lett.*, vol. 33, no. 7, pp. 571-573, 1997.
- [17] D. Biolk, J. Cajka, K. Vrba, V. Zeman, "Nth-order allpass filters using current conveyors", *J. Electr. Eng.*, vol.53, no.1-2, pp.50-53, 2002.
- [18] C. M. Chang, A. M. Soliman, M. N. Swamy, "Analytical synthesis of low-sensitivity high-order voltage-mode DDCC and FDCCII-grounded R and C all-pass filter structures", *IEEE Trans. Circuits Syst. I : Regular Papers*, vol.54, no.7, pp.1430-1443, 2007.
- [19] M. Koksall and M. Sagbas, "A versatile signal flow graph realization of a general transfer function by using CDBA," *Int. J. Electron. Commun. (AEU)*, vol. 61, pp. 35-42, 2007.
- [20] K. Ogata, *Modern Control Engineering, Fourth-Edition*, Prentice-Hall International, Inc., Upper Saddle River, New Jersey 07458, 2002.
- [21] M. E. Van Valkenburg, *Analog Filter Design*, Oxford University Press, Inc., New York, New York 10016, 1982.
- [22] M. A. Soderstrand and S. K. Mitra, "Sensitivity analysis of third order filters", *Int. J. Electron.*, vol.30, pp.265-272, 1971.
- [23] W. Tangsrirat, O. Onjan, T. Pukkalanun, "SFG synthesis of general n^{th} -order allpole voltage transfer functions using VDAs and grounded capacitors", *Proc. Forth Joint Int. Conf. Information Commun. Tech., Electron. Electrical Eng. (JICTEE-2014)*, Chiang Rai, Thailand, 5-8 March, pp.291-294, 2014.

Understand True Lightning Protection Neutralize The Environmental Climate

Witsarut Assawachatsakul and Krischonme Bhumkittipich
Power and Energy Research Unit
Department of Electrical Engineering, Faculty of Engineering
Rajamangala University of Technology Thanyaburi
E-mail: witsarut_a@rmutt.ac.th

Chatchom Sucharitsopit
ITAC Innovation Co., Ltd., 170 Piman Village, Nongbon,
Pravet, Bangkok10250, THAILAND,
Email:chatchom@itacinnovation.com

Abstract— The studies of natural lightning cannot just rely on laboratory experiment, for it is impossible, in any way to the extreme difficulty, to recreate all the factors and keep track of all the parameters that cause natural lightning. It need to be of the "exploration" type and the classification of data, as consequence, of "epidemiological" type that is of an historical-statistical type over a proper number of plants especially in areas of high keraunic danger and where natural lightning attracting systems have previously failed, and for a proper period of time. Present measurements indicate that an average of almost 1 A of current flows into the stratosphere during the active phase of a typical thunderstorm. Therefore, to maintain the fair weather global electric current flowing to the surface, one to two thousand thunderstorms must be active at any given time. There is, therefore, great motivation to develop effective countermeasures against the destructive effects of weather, and, conversely, to enhance the beneficial aspects. This paper will present the concept on designing absolute lightning protector which will in turn present the understanding of fair weather control through lightning protector that will benefit the human life.

Index Terms-- Atmospheric electricity; Lightning Protection; Absolute Lightning Protector; Weather Control; Electromagnetic Radiation; Thunderstorms; Human Life.

I. INTRODUCTION

From NASA research, Stratospheric lightning could potentially deposit significant energy into the stratosphere, causing important chemical perturbations. In addition, these lightning events may generate strong electric fields and electromagnetic pulses which might interact with the Earth's ionosphere and magnetosphere. Finally, strong fields at high altitudes may generate runaway electrons which could then produce high energy x-rays and even gamma rays. Thus, it is possible that lightning may generate electromagnetic radiation, ranging from extremely low frequency to gamma radiation. Rainfall is at the heart of Earth's unique ability to sustain life as we know it. On the global scale, heat released by the condensation of water vapor is a principal cause of motion in the atmosphere. Tropical rainfall, due to its abundance, plays a significant role in this process. The earth's weather has a profound influence on

Corresponding Author : witsarut_a@rmutt.ac.th

agriculture, forestry, water resources, industry, commerce, transportation, construction, field operations, commercial fishing, and many other human activities. Adverse effects of weather on man's activities and the earth's resources are extremely costly, amounting to billions of dollars per year, sometimes causing irreparable damage as when human lives are lost in severe storms. The scientists found that during fair weather, a potential difference of 200,000 to 500,000 Volts exists between the Earth's surface and the ionosphere, with a fair weather current of about 2×10^{-12} amperes/meter². It is widely believed that this potential difference is due to the world-wide distribution of thunderstorms. It is based on Empiricism, the method by which we gain knowledge through observation and measurement. Traditionally they think of the scientific method comprising the following stages.

- 1 Observation
- 2 Hypothesis
- 3 Prediction
- 4 Testing.

An Actuality approach works backwards from observation, and takes a broad approach to science. Birkeland, for example, believed in experimentation and observation in addition to mathematical modeling, despite having trained as a mathematician.

It is therefore to truly understand how absolute lightning protection neutralize the environmental climate is to be of the "exploration" type and the classification of data, as consequence, of "epidemiological" type that is of an historical-statistical type over a proper number of plants especially in areas of high keraunic danger and/or where natural lightning attracting systems have previously failed, and for a proper period of time. There are many studies proving that electric forces assert themselves in upsetting the sensitive balance and causing precipitation in the ionosphere. During the last century a much improved form of lightning protector characterized by the employment of a terminal of considerable area and large radius of curvature was made which makes impossible undue density of the charge and ionization of the air. These protectors act as quasi-repellents, and so far have never been struck the vicinity though exposed a long time. Their

safety is experimentally demonstrated to greatly exceed that invented by Franklin.

Once the true science of lightning protection to neutralize the environment climate is understood, *fair weather control* then can be created and help to sustain life. The earth's weather has a profound influence on agriculture, forestry, water resources, industry, commerce, transportation, construction, field operations, commercial fishing, and many other human activities. Adverse effects of weather on man's activities and the earth's resources are extremely costly, amounting to billions of dollars per year, sometimes causing irreparable damage as when human lives are lost in severe storms.

II. THE STUDY

The initial design of the lightning protection in this study was based on the needs to increase the effectiveness of the Franklin Rod installed worldwide. The effectiveness of the design was explicit according to the reference sites installed nationwide throughout the century as per Appendix. The design as per Fig. 1 comprises of a franklin rod and a sphere connected together via impedance.

The franklin rod is connected to the earth wire while the sphere is floating. According to many studies, from Tesla discovery, Franklin Rod actually aids the lightning in hitting the building because the rod helps in ionizing the surrounding air [1]. Tesla then referred to Culomb's law which is the quantity of electricity per unit area, electrical density, increases as the radius of curvature of the surface is reduced. Moreover, the accumulated charge created an outward normal force equal to $2\pi \times D^2$. D is the density. When the charge density exceeds Electron density $2.6 \times 10^8 \text{ cm}^{-3}$, the corona will form [2].

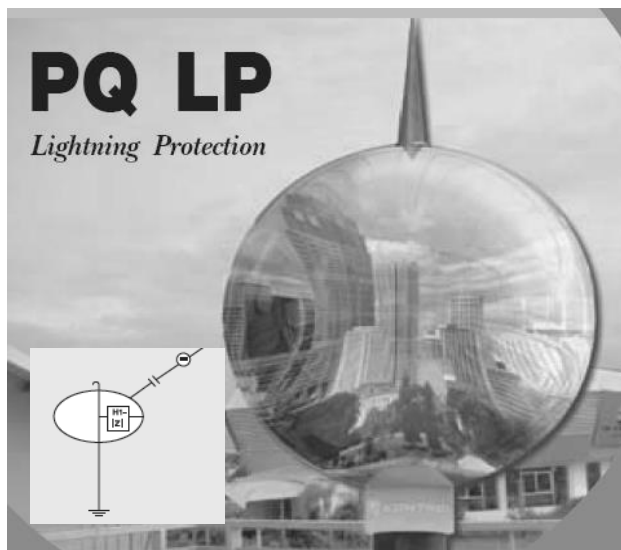


Fig. 1 Design of Absolute Lightning Protection [1]

Table 1 Atmospheric discharge characteristics at ground level

Parameter	Glow Corona	Streamer	Leader
Temperature	~300 K	~300 K ^[14]	> 5000 K ^[9, 15]
Electron energy	1-2 eV ^[4]	5-15 eV ^[15]	1-2 eV ^[18]
Electric field	0.2-2.7 kV/cm ^[10]	5-7.5 kV/cm ^[15]	1-5 kV/cm ^[9]
Electron density	$2.6 \times 10^8 \text{ cm}^{-3}$ ^[3]	$5 \times 10^{13} - 10^{15} \text{ cm}^{-3}$ ^[9, 15]	$4 \times 10^{14} \text{ cm}^{-3}$ ^[13]

Table 1 shows Atmospheric discharge characteristics at ground level. Corona discharge is an electrical discharge brought on by the ionization of a fluid surrounding a conductor that is electrically energized. The discharge will occur when the strength (potential gradient) of the electric field around the conductor is high enough to form a conductive region, but not high enough to cause electrical breakdown or arcing to nearby objects. It is often seen as a bluish (or other color) glow in the air adjacent to pointed metal conductors carrying high voltages. When the air near the point becomes conductive, it has the effect of increasing the apparent size of the conductor. Since the new conductive region is less sharp, the ionization may not extend past this local region. Outside this region of ionization and conductivity, the charged particles slowly find their way to an oppositely charged object and are neutralized. This is the cause of inefficacy of Franklin Rod. It is obvious that such may happen at a comparatively low pressure if the conductor is of extremely small radius or pointed. The corona effect prohibits the upstream to capture the downstream lightning while the nearby sharp structure generates the upstream and is struck. To reduce the effect, the outer sphere is added to reduce the corona effect by discharging the corona ions. The sphere secures a very low density and preserves the insulating qualities of the ambient medium.

This lightning design was then tested in various areas in the country as Table 2. The results have been very astonishing. There has never been single report of failure after 10 years of more than 100 terminal installations even in the area of very high lightning phenomenon in the southern part of Thailand at Petroleum Authority of Thailand's tank farm. There was one occurrence reported by an officer at the PTT Songkhla that he saw lightning strike on the lightning terminal installed near one tank but there was no either damage or strike on any tanks.

From this result over period of time, it is proven that Tesla discovery of lightning protection concept was right, the terminal construction can suppress charge emission. Therefore it is to further explore this knowledge for the better of human life on fair weather control. "Fair weather electricity deals with the electric field and the electrical current in the atmosphere, and the conductivity of the air," explained Dr. Lothar Ruhnke of Airborne Research Associates in Weston, Mass. The cause of all the storms in every region is the result of ion asymmetry (unstable atmospheric conditions). From modern observations, it can be seen that changes in the weather are often associated with pronounced changes in the mean and variability of the Potential Gradient as noted originally by early workers in atmospheric electricity.

Table 2 Some Thailand reference sites of lightning protection installation

Year	Region	Organization
1999	Central	Armed Forces Academies Preparatory School
1999	Central	Rubber Research Institute
2000	Bangkok, Central, Southern, Northern, Eastern	Petroleum Authority of Thailand
2001	Southern Island	Private company
2003	Bangkok	Bangkok Metropolitan Authority
2004	Northeastern	Air Forces
2006	Central	Office Building, Condos, Factories

Potential Gradient	negative		positive		
	<-2000 V/m	-500 V/m to +50 V/m	+100 V/m	+150 V/m to +200 V/m	+200 V/m to +1000 V/m
Variability in Potential Gradient	DISTURBED WEATHER		FAIR WEATHER		DISTURBED WEATHER
negligible (±5%)			clean maritime air		fog
small (±10%)					polluted continental air
moderate (±20%)			steady rainfall		snow
substantial (±50%)	non-precipitating convective cloud				
large (±100%)	Heavy shower/thunderstorm				Heavy shower/thunderstorm

Fig. 2 From Weather articles: Atmospheric electricity in different weather conditions by A. J. Bennett and R. G. Harrison Department of Meteorology, University of Reading [3]

To stabilize the Potential Gradient for fair weather conditions, the potential must be kept at +100V/m to 200V/m. In the previous century Kelvin suggested a model of the earth's atmosphere as a giant capacitor, with the ionosphere and ground as its plates. As per LL. Williams papers [4], to understand the variation with height of electrical properties between ground and ionosphere, consider the conductivity of the intervening atmosphere. The atmospheric density decreases exponentially with height h:

$$n \propto e^{-h/H_0} \tag{1}$$

where H_0 is about 8 km. With a finite conductivity and an electric field, current must flow. In steady state, this current must be constant with height; otherwise charge would build up to catastrophic levels at one height or another, contradicting the assumption of steady state. Invoking Ohm's law for constant current density

$$J = \sigma JE \tag{2}$$

(Ignore vector behavior of E, and consider only vertical currents and fields):

$$E \propto e^{-h/H_1} \tag{3}$$

The electric field decreases exponentially with height, and the strongest field magnitude occurs right at the surface. Now, since the electric field is varying exponentially with height, it will have a finite divergence. And Gauss' law tells us that a divergence in the electric field implies a charge density ρ :

$$dE/dh = \rho/\epsilon_0 \tag{4}$$

Therefore we also have a net space charge density existing in the atmosphere which vanishes approaching the ionosphere, and increases exponentially toward the ground. At the ground,

$$\rho_0 = E_0\epsilon_0/H_1 \cong 2 \times 10^{-13} \text{ C/m}^3 \tag{5}$$

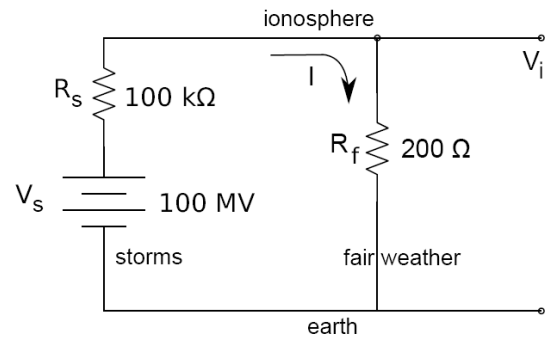


Fig.3 The global electric circuit

A typical lumped-element circuit for this region is shown in Fig.3 [5]. The model is arranged vertically, with the earth at the bottom and the ionosphere at the top. Both the earth and the ionosphere are very good conductors compared to the atmosphere, so they can be considered as equipotential. The values of the circuit elements shown in the figure are typical, but can vary with time of day, season, and location.

The aforementioned study leads to the fact that the lightning protection in this study, with the spherical shape, will prevent the concentration of the ions in the cloud but the central pointed rod will help direct the strike to preferred point because it has been known since 1931 that the reason lightning behaves the way it does is the existence of randomly-distributed space charge in the atmosphere. That space charge governs the development of the lightning channel over most of its route, and they blind it to the existence of ground objects. Under the ordinary weather conditions, when the sky is clear, the total amount of electricity distributed over the land is nearly the same as that which would be contained within its horizontal projection.

III. THE APPLICATION

To further prove the application of the study, more installation to collect the statistical data is required for full understanding of the discovery. However, the capability of any given equipment need not be greater than area concern and these depend, partially, upon the character of the landscape proximate to the building site.

In times of storm, owing to the inductive action of the clouds, the immense charge may be accumulated in the area. The density is greatest at the most elevated portions of the ground. The density at the terminal end should be inversely as the radius of curvature of the surface. The terminal surface therefore must be of large radius of curvature and sufficient area to make the density very small and thereby prevent the leakage of the charge and the ionization of the air. The data collected should show the relation of the sphere radius and the coverage protection together with the potential gradient measured. Also the lightning counter should be attached to log the number of lightning strikes the terminal. The historical data of the weather conditions of the areas should also be accumulated for comparison.

IV. CONCLUSION

The absolute lightning protection design should not be only the pointed rod which induces corona effect causing the ionization of the vicinity atmosphere and making the rod inefficacy. The terminal surface must be of large radius of curvature and sufficient area to make the density very small and thereby prevent the leakage of the charge and the ionization of the air. The spherical design of the terminal will reduce the immense charge in the cloud while the pointed rod in the center will, in case of unexpected circumstance; help direct the strike to preferred point. However, most of the time, the spherical design terminal will maintain the fair weather condition potential gradient to reduce the damages caused by the severe storm and improve the rainfall to sustain human life.

REFERENCES

- [1] Tesla Has New Pointless Lightning Rod, *Electrical Experimenter*, October, 1918.
- [2] J. A. Rioussset, Fractal modeling of lightning discharges, Master's thesis, The Pennsylvania State University, University Park, PA (2006).
- [3] A. J. Bennett and R. G. Harrison, Weather articles: Atmospheric electricity in different weather conditions, Department of Meteorology, University of Reading.
- [4] L.L. Williams, Electrical Properties of the Fair-weather Atmosphere and the Possibility of Observable Discharge on Moving Object, January 1999.
- [5] Joseph M. Crowley, Electrostatic Applications, The Fair-Weather Atmosphere, *Power Source, Proc. ESA Annual Meeting on Electrostatics 2011*, Paper A2

Enhancing Power Electronics and Grid Converter Laboratory Based on Embedded System

C. Tarasantisuk and E. Anusurain

Department of Electrical Engineering, Rajamangala
University of Technology Krungthep,
2 Sathorn, Bangkok, Thailand
Email: chanrit.t@rmutk.ac.th

T. Suyata

Department of Electrical Engineering, Rajamangala
University of Technology Thanyaburi, Thanyaburi
PathumThani, Thailand
Email: thongin.ee@gmail.com

Abstract— In this paper, an experimental tool for teaching power electronics and grid converter laboratory is achieved with using embedded system. Department of Electrical Engineering, Rajamangala University of Technology Krungthep (RMUTK) teaches students in power electronics and electric drives. It is also necessary to learn about basic systems and demonstration. This paper will discuss the basic power electronic courses with an enhancing Power Electronics Laboratory based on Embedded System. It is using Waijung blockset and compiler code from host to STM32F497 target with embedded coder in the Matlab/Simulink environment.

Keywords— Power Electronics, Grid Converter, Embedded System and Waijung Blockset.

I. INTRODUCTION

In presently, the growing of several products in the field of electric applications has extended and covered with a wide range of customers [1], [2], [3], [4]. The appliances are also designed for respond market demand and end user demand. It is possible that the applications rapidly continue to extend in appliance areas such as lamp controls, power converter for motor drives, factory automation, transportation, energy storage, multi mega-watt industrial drives, and electric power transmission and distribution. So, the power electronics was intended to learning in role plays most important for education.

The enhance laboratory using some section for discuss modeling concept, simulation concept, and experimental concept. Frist, these procedures can help understanding with all system operating. The waveforms make form hardware that student can access measurement and seem all completely. In addition, the objective studies of a final class would like demonstrated all a practically good experience. Future, tools intended using creative work or new generate idea essentially; it can be helping application works that very easy to control power electronics circuit in embedded system process.

The greater efficiency processor improves together futures power electronics technology. The studies would be attractive opportunities for new technology and interfaces that enable integration on the laboratory. The operation work of processor and hardware, we would like to point out that the tool could also support the control techniques in laboratory practice, with a result of improving the experimental probably new generate

ideas to difference among the groups for the mini project of engineering.

II. THE LABORATORY OBJECTIVE

The classification about objective to learned power electronic laboratory:

- Basic of RTW and Waijung Blockset with an Emulator System
- Buck dc to dc converter with PWM Blockset
- Single Phase Inverter
- Three-Phase Inverter with SPWM
- Advanced PWM for Three-Phase Inverter
- Mini Project

III. THE SETUP LABORATORY

A. Hardware and controller

The digital controller had been used implementation using low-cost micro controller from ST microelectronics STM32F407VG (STM32 Discovery) evaluation board with specifics of Features: ARM 32-bit MCU, 210D MIPS/1.25 DMIPS/MHz 1MB Flash memory/192+4KB on-chip RAM [5].

B. Waijung blockset

The waijung blockset is free software tool from Aimagin company that provided for embedded education and application [6]. The benefits of low-cost product and can be an experiment rapidly. Moreover, it had been covered and appropriated for students begin the education in power electronic and control system. It provided for connecting to the simulink model directly. Application models can be used to easily and automatically generate C code from Matlab/Simulink model into STM32 Discovery microcontrollers (Targets). A Waijung software for generating and compile C code from Matlab/Simulink model, There's basically required other including Simulink Coder and embedded Coder. An embedded used GNU ARM for compiling the source code systems. The configuration setup that following.

In a first step, update diagram on the menu bar : Simulink application models for using show in Fig.1, Waijung target setup blockset will be recalled configuration model and checked time profiler of the application model. Results generation systems will be reported the sample time legend of route color line with many colors on sample rate model.

In a second step, build diagram on menu bar of Fig 2, Waijung track build process will be accessed to Simulink blockset library, STM32 peripherals, manage peripherals data, generated code and downloaded on the target with connecting to U-ART communication. STM32 ST-LINK utility user interface show in Fig. 3.

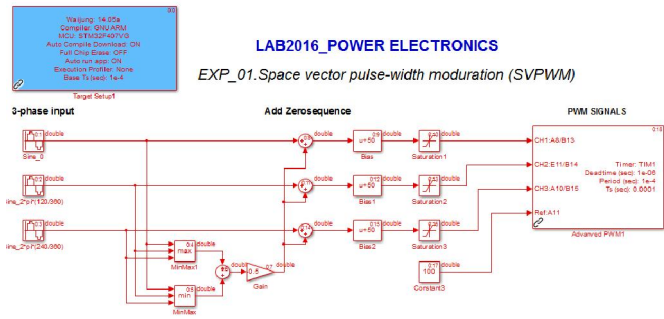


Fig 1. Waijung blockset and Simulink model.

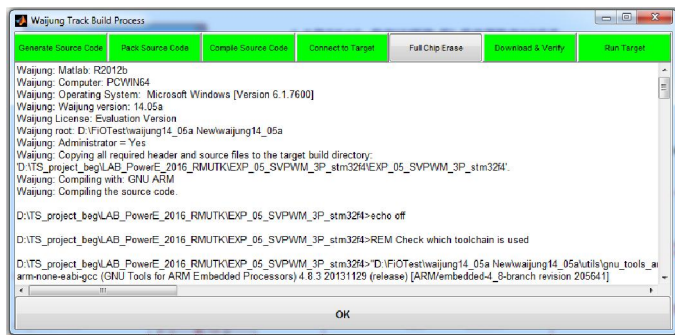


Fig 2. Waijung build process.

C. Dc to ac converter

The dc to ac power converter is the technology that accesses the efficient and flexible interconnection to difference items in the electric power system [2], [4], [8], [9]. Hence it is keys element of center convert dc voltage to ac voltage, inverter is based on semiconductor element and control technology. And the transient behavior output voltage depends on difference filter types. The ratio modulations are factor provided to an output voltage level. This educational attended the power converter with effectively covered constructing both three phase inverter and single phase inverter experimental. In principles of studies had knowledge basic electric circuit and machine clearly used analysis switching state analysis coupling with each type loads.

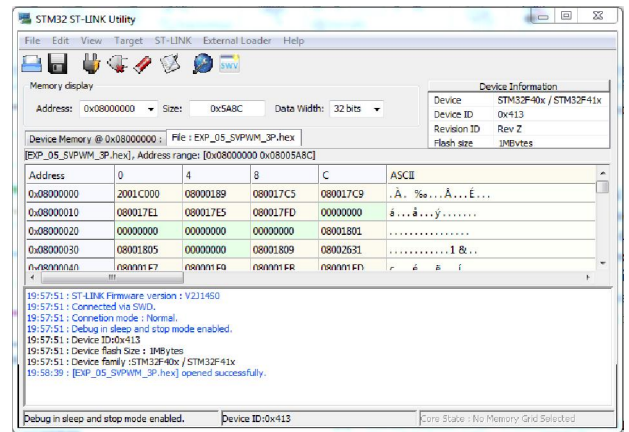


Fig 3. STM32 ST-LINK utility user interface.

The details are presentation of three phase inverter and single phase inverter with an enhancing power electronic laboratory device. Student opportunity access an ac waveform from output circuits with monitoring on oscilloscope, ac waveform can help to comprehend characteristic each pattern switch. Before an experiment, they must be findings operate systems with placing circuit base on simulation and results suggests nearly characteristic switch, output waveforms after, voltage waveforms of these circuits. After, we will discuss general switching concept with half bridge and full bridge type. Basic pulse width modulation blockset are benefited for generation signal that complementary achieved both high and low signals. The designer of voltage output depend on ratio modulation, they are determined value modulator form handout laboratory. The appropriate rate value notching filters provide reducing harmonics distortion and quality wave forms output. A student will meet design and practical in an experiment. The details of power electronics includes:

- General concept
- Basic principles/concepts
- Single-phase inverter
- Basic single phase pulse width modulation blockset
- Notching filter
- Harmonics
- Modulation.
- Three-phase inverter
- Advance three phase pulse width modulation blockset

D. Dc to dc converter

Dc to dc converters such as boost converter, buck converter, and buck – boost convert. These are very often used application of all converters [2], [4]. There is a basic transferring energy only one direction. An experiment requires studying basics converter topologies in switch mode dc power supply and basic pulse width modulation blockset in embedded system. The modulator provided Waijung blockset for a

generation PWM signal from a basic comparison between dc value and triangle wave.

The switching frequency output of target used to control switch of the circuit. So, in session brief a buck converter (step-down converter) used to learning the basic power electronic, detail of this section includes:

- The fundamental operation of power electronic converter.
- Switching characteristics of dc to dc converter.
- Switching comprehensions of cont/discont conduction mode.
- To be able to analyze and design a low pass filter.
- To be able to analyze and design simple power electronic converter.
- To give the students an appreciation the current state of an electronic circuit.
- To provide a regulated output voltage.

Buck dc to dc converter, we are design circuit and make PCB without inserting the components on a board. The student will have been conversion concept and theory from after the lecture session for calculating all element electronic converters. The specific designer required such as power input, power output, requited current mode, switching frequency and duty ratio.

E. Control designer with Matlab/Simulink

This section outlines basic goals for example design close loop control in embedded system [10], [11], [12]. This experiment requires the student to construct a simple design loop control of buck dc to dc converter. According to the structure of the control block diagram in fig.4, it illustrates a simple structure of control block diagram for the buck converter. It consists three block diagram, first controller part is PI controller for used regulate output voltage from switching switch, there are compared and compensated both signals a between reference voltage and an output voltage of output power circuit, main control duties are forced voltage output keep tracking reference voltage command. Second, time delay part is using for signal processing of main microcontroller unit processor. The time interval of all process should be adequate time computing for overall loop control.

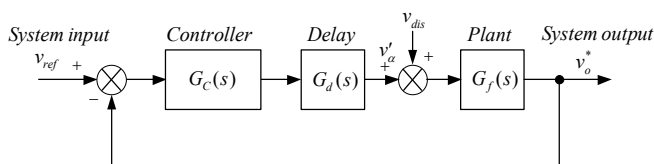


Fig 4. Control block diagram of the buck converter.

In additional part, low pass filter of an output circuit, for dc to dc converter, designing from required output power with

traditional depend on continuous conduction mode of a circuit. The open loop transfer function for a circuit can be express as

$$G_{ol}(s) = G_c(s)G_d(s)G_f(s) \tag{1}$$

In this design, when students should be selected the value of parameter from table 1, From Equation 1, Continuous-time transfer function can be conversion to discrete-time transfer function (c2d) with C2D with sample time: $6.25e^{-05}$, low pass filter transfer function becomes

$$G_{ol}(s) = \frac{0.001154z^3 + 0.002743z^2 - 0.002902z - 0.0007584}{z^4 - 3.381z^3 + 4.216z^2 - 2.284z + 0.4495} \tag{2}$$

In practical to ensures stability student must design and draw a bode plot graphic of the open loop transfer function. Guideline for example design, we should design in same manner, where 1.5 and 500 are the proportional gain and integral gain respectively. The results are generally present in Fig.5, show Bode plot graphic serve adequate phase margin = 52° and gain margin = 13.2 dB , bandwidth system is about 418 rad/s .

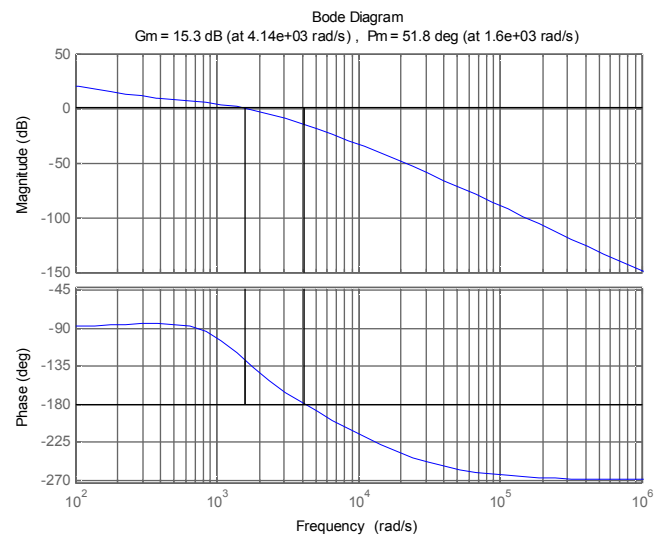


Fig 5. Bode plot of close loop buck converter.

In Fig. 6, result from an output fast dynamic responds to the step commanded of feedback control. It can be track and changed abruptly at settling time up to 0.006 s , which indicate that in order to verify the close loop control method can be achieved using the proposed control scheme. Moreover, in Fig 6 show to respond to loop feedback control of buck converter plant with real time work shop (RTW) emulator system, student will be learned basic emulator system with Waijung blockset.

It is to be mentioned to different type controller. So, the student will be comprehensions and suggestion about characteristic of each controller.

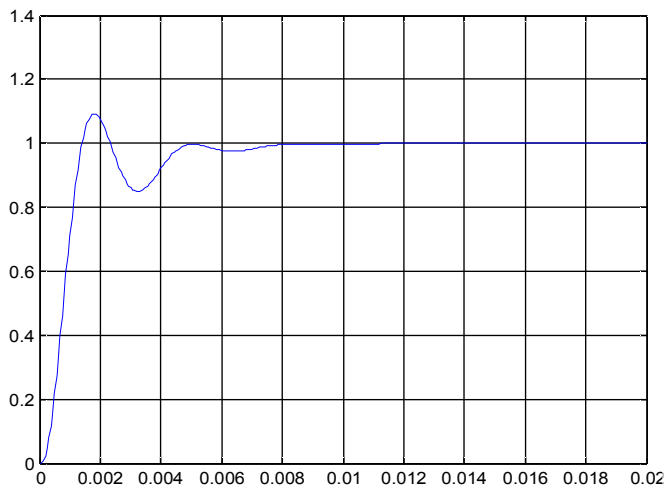


Fig 6. Respond to step commanded of buck converter.

F. Standalone Single phase inverter

Today, many renewable energy sources as an alternate energy source is becoming most popular such as solar, wind, mini-hydro, and tidal power [1]. However, for example, apply to an application on a section. Solar and wind power intended more than other energy sources as both are systems worldwide and can be using the combination with power electronic technology. When we considered applying for planning application, PV solar is very high impact more than wind such as small, quiet, low cost. Moreover, it can be generating dc power supply board directly. The following factors appropriated to mini project for single phase standalone inverter applications [1]:

- Simplifies for the comprehensible studies.
- Basic topology dc to ac converter.
- Low-level dc voltage (student safety)
- To be able access results from a circuit traditional.
- Rapidly for set-up and measuring experimental.

Fig.7 shows the fundamental device of power electronics laboratory. The dc bus had been using 42 volt. The STM32F407 microcontroller with Waijung blockset is used to generate a PWM signal and digital controller. Dc bus voltage for an inverter is created for safety and saved energy consume power when the test in a laboratory. The inverter board constructed from integrated circuits the isolate gate driver, MOSFETs, voltage and current sensors.

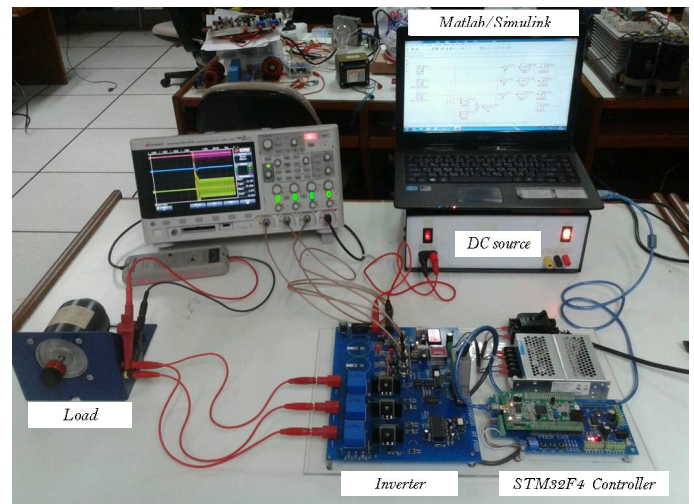


Fig.7 Power Electronic laboratory based on embedded system at Rajamangala University of Technology Krungthep (RMUTK).

IV. LABORATORY EXPERIMENTAL RESULTS

In order to demonstrate the effectiveness of proposed Standalone single phase inverter mini project bases on Enhancing Power Electronics Laboratory with Embedded System. The practical regulated the current command with proportional integral control. It contained discretized system. The experiments are carried out using Matlab/Simulink and STM32F4, respectively. Also, PV arrays as an input dc to dc converter used a dc power supply, loading used testing with connected resistor directly to the VSI. The inverter designed was tested under different dynamic current command conditions. The experimental hardware setup and system block diagram for PV inverter is shown Fig. 7 and Fig. 8, respectively.

The proposed buck converter that reasonable way to clearly identify the system parameter with a boundary of continuous conduction mode operation. Keys waveform 9, shows the waveforms for v_g and i_L of inductor designed current continuous mode. When consideration in steady state condition achieved that ripple current switching in transient condition and steady state condition are good smooth transitions.

Fig.10 show the waveforms of low pass filter with LC element. In this case show measured from output filter between an output inverter and resistive load. These result in case studies of low pass filter topology reports with key waveform that u-phase voltage and current are in-phase completely.

Results in Fig.11, the good performance of loop control system are responsibility during various current commands of grid converter mini-project. When step command changed abruptly, close loop control designed provides smooth transitions and fast response without

oscillation of current waveforms. And serve little error, indicated by taking the current command and current measured.

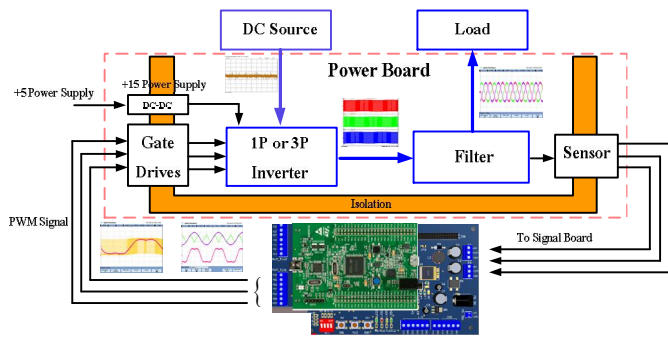


Fig.8. The power electronics laboratory system block diagram.

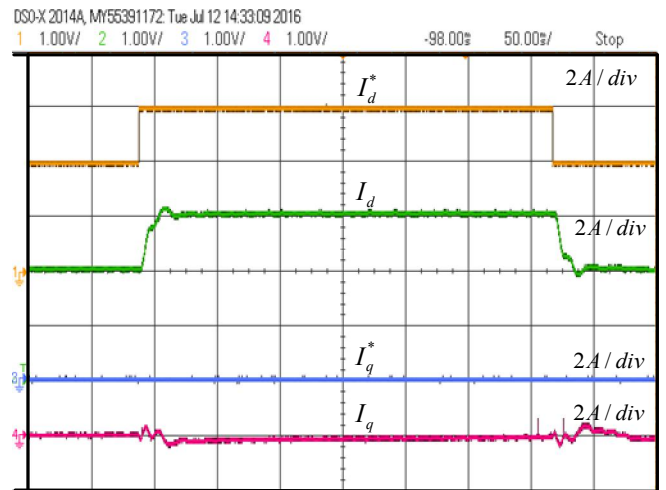


Fig.11 Current waveforms of grid inverter with step change current command.

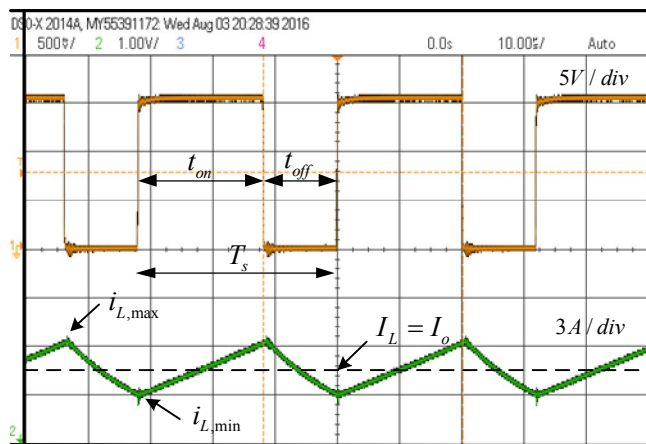


Fig.9 Current at boundary of continuous conduction mode.

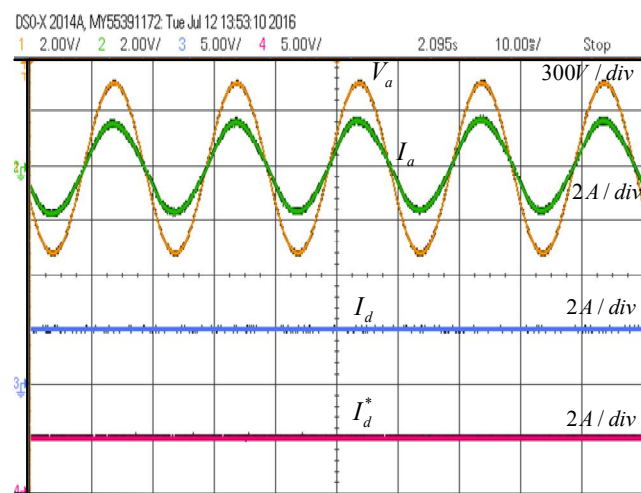


Fig.10 Phase voltage and current of single phase grid inverter.

V. CONCLUSIONS

This paper presents an experimental tool in teaching power electronics and grid converter laboratory is achieved with used embedded system. It is very easy to demonstrate the learning process. And it can reduce time in the process more than to the conventional system for teaching, and it is very easy to experiment. Moreover the educations these can be adaptable to engineering project or application with renewable energy systems and industrial products.

REFERENCES

- [1] C. C. Chan, and K. T. Chau. "An overview of power electronics in electric vehicles." IEEE transactions on Industrial Electronics 44.1, 1997, pp. 3-13.
- [2] R. Teodorescu, and M. Liserre. "Grid converters for photovoltaic and wind power systems." vol. 29. John Wiley & Sons, 2011.
- [3] D. A. Torrey, "A project-oriented power electronics laboratory." IEEE Transactions on Power Electronics 9.3 (1994) pp. 250-255.
- [4] N. Mohan and T. M. Undeland. Power electronics: converters, applications, and design. John Wiley & Sons, 2007.
- [5] http://www.st.com/content/st_com/en/search.html?q=stm32f4discovery-t=keywords-page=1
- [6] <https://www.aimagin.com/products/fio-boards.html>
- [7] R. W. Erickson and D. Maksimovic "Fundamentals of power electronics" Springer Science & Business Media, 2007
- [8] Y. Amirnaser and I. Reza "Voltage-Source Converters in Power Systems", Wiley, 2010
- [9] Y. Xue, et al. "Topologies of single-phase inverters for small distributed power generators: an overview." IEEE Transactions on Power Electronics 19.5, 2004, pp. 1305-1314.
- [10] L. Guo, J. Y. Hung, and R. M. Nelms. "Digital controller design for buck and boost converters using root locus techniques." Industrial Electronics Society, 2003. IECON'03. The 29th Annual Conference of the IEEE. vol. 2., 2003
- [11] C. L. Phillips and R. D. Harbor., "Basic feedback control systems", Prentice-Hall, Inc., 1991.
- [12] E. Twining and D. G. Holmes, "Grid current regulation of a three-phase voltage source inverter with an LCL input filter," IEEE Trans. Power Electronics., vol. 18, no. 3, pp. 888-895, May 2003.

Infection Renal Dialysis Detective Medical Devices from Idea to End Users

Kesorn Pechrach Weaver

R&D Department
Ronsek Limited
Bishops Stortford, UK, CM23 5LE
E-mail: kesorn.pechrach@ronsek.com

Abstract - The kidney structure, function and blood vessels inside are complex. The glomerular capillary is about 5-10 μm in diameter, which could be blocked easily and progress into chronic kidney failure where the renal function has permanent loss. This paper presents the physical properties of blood vessels can be simulated by electrical (R, L, C) circuit models

It is shown that the renal blood vessels indicate that the resistance is greatest at a section of the segmental artery, the blood flow starts to reduce the speed at this section, where the blood pressure drop occurs. The arcuate artery has a higher elasticity, which has the highest capacitance than the others.

It is demonstrated how to develop from the idea to be the product for the end users, starts with addressing a problem, confident in the technology and in economically.

Keywords — Kidney failure; renal blood vessels; electrical kidney; renal vascular impedance.

I. INTRODUCTION

After decades of frustration, it has been thought that this kidney dialysis medical device can be a smaller and cheaper infection detector which able to measure cloudy liquid and colours, temperature rising, flow draining speed and dialysis duration. Afterward, these data send via mobile phone direct to doctor, consultant or specialist in the renal hospital.

The renal blood flow is very important for the kidney function to maintain the physical condition of the body. Blocked renal blood vessels could cause acute kidney failure. This could progress into chronic kidney failure where the renal function has permanent loss. The glomerular capillary is about 5-10 μm in diameter and could be blocked easily. Current treatments are dependent on drugs only, but there is current interest in the application of nanotechnology in the development of alternative treatment strategies. [1].

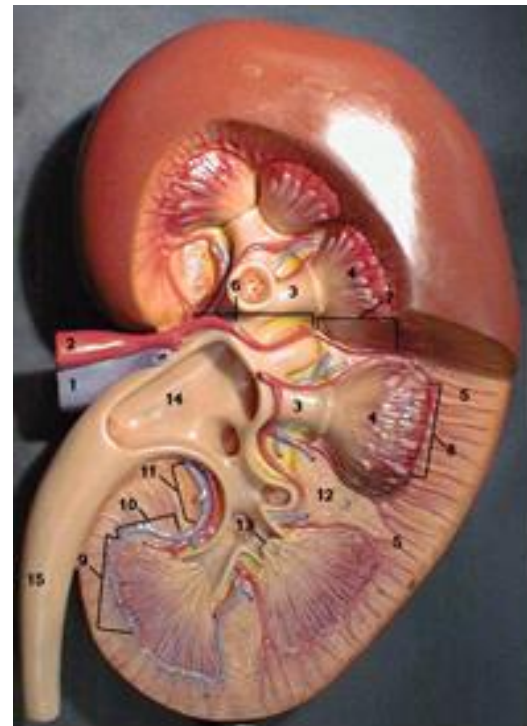


Figure 1: shows the kidney details: whereas 1) renal vein, 2) renal artery, 3) renal calyx, 4) medullary pyramid, 5) renal cortex, 6) segmental artery, 7) interlobar artery, 8) arcuate artery, 9) arcuate vein, 10) interlobar vein, 11) segmental vein, 12) renal column, 13) renal papillae, 14) renal pelvis, 15) Ureter

II. RENAL VASCULAR SYSTEM AND METHODS

Electrical circuit elements were used to simulate the properties of blood vessels. Hill et al [2] used to load model to simulate the umbilicoplacental circulation. However, the renal blood vessels impedance should provide more physical information on the properties of the renal system.

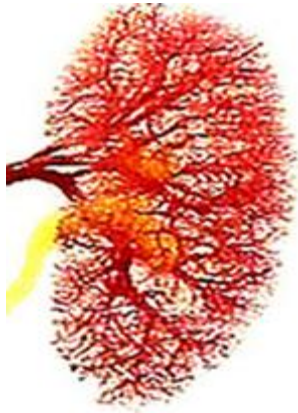


Figure 2: shows renal blood vessels [3]

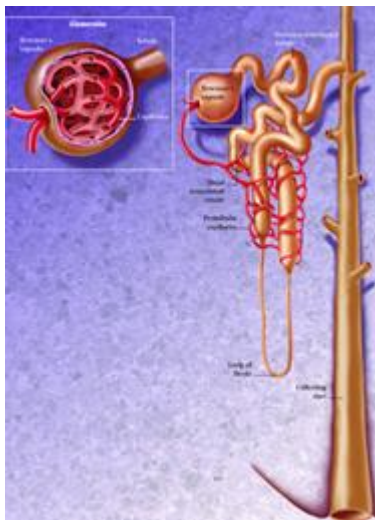


Figure 3: shows details in glomerular capillary structures [3]

The physical properties of blood vessels can be simulated by electrical (R, L, C) circuit models [4]. The electrical voltage (V) and electrical current (I) are used as analogues of the blood pressure (P) and blood flow (Q). The model shown here consists of five blocks, each block with resistance (R), series inductance (L) and parallel capacitance (C) as shown below:

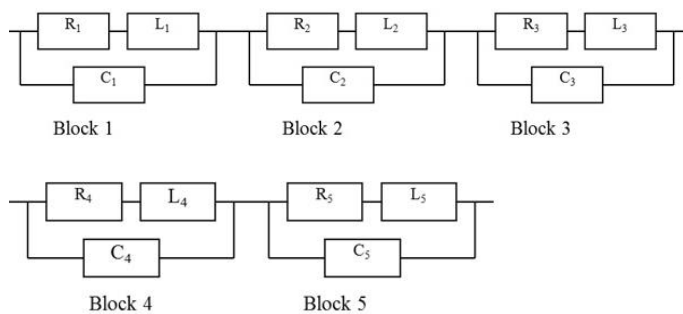


Figure 4: Five blocks electrical model for renal vascular impedance

$$Z(\omega) = \left(\frac{R_1 + j\omega L_1}{(1 - \omega^2 L_1 C_1) + j\omega R_1 C_1} \right) + \left(\frac{R_2 + j\omega L_2}{(1 - \omega^2 L_2 C_2) + j\omega R_2 C_2} \right) + \left(\frac{R_3 + j\omega L_3}{(1 - \omega^2 L_3 C_3) + j\omega R_3 C_3} \right) + \left(\frac{R_4 + j\omega L_4}{(1 - \omega^2 L_4 C_4) + j\omega R_4 C_4} \right) + \left(\frac{R_5 + j\omega L_5}{(1 - \omega^2 L_5 C_5) + j\omega R_5 C_5} \right) \quad (1)$$

$\omega = 2\pi f$ where f is the frequency of heart beat at 72 beats/min.

III. RESULTS AND DISCUSSION

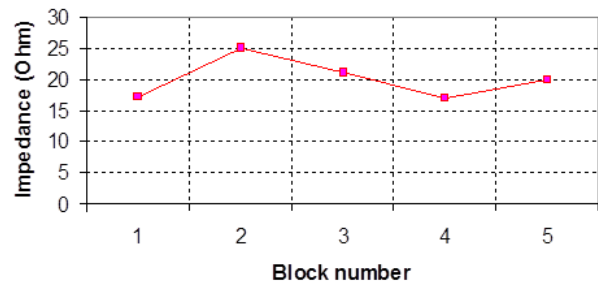
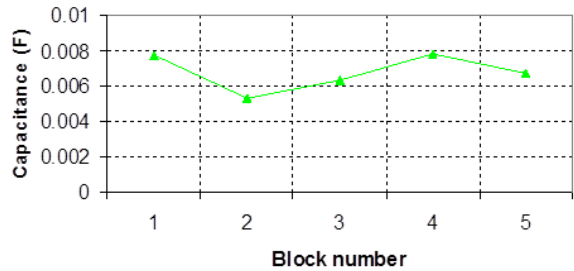
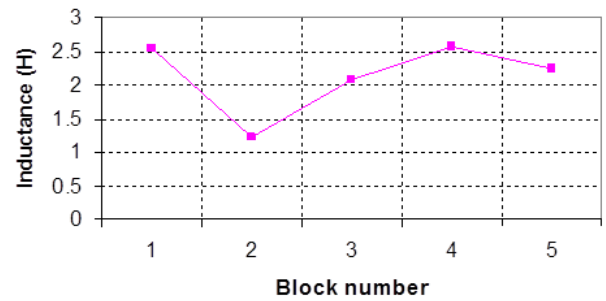
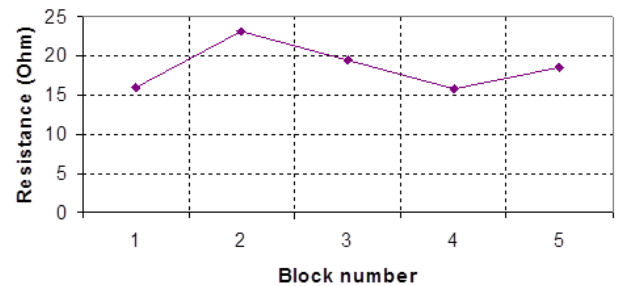


Figure 5: Renal vessel model results: resistance, inductance, capacitance and impedance

The profile of resistance is shown similar to the waveform of impedance. Block 2 has the highest resistance, but lowest capacitance and inductance. Block 4 has the lowest resistance, however, it is the highest capacitance and inductance.

The model parameters of the renal blood vessels indicate that the resistance is greatest at a section of the segmental artery. This indicates that the blood flow starts to reduce the speed at this section. This agrees with the conclusions of Guyton [5] where the blood pressure drop occurs in the smaller artery. The large capacitance could indicate higher elasticity [6]. Thus, the arcuate artery could have a higher elasticity than the others.

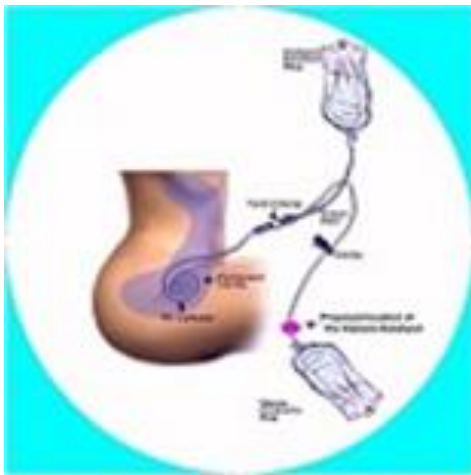


Figure 6: CAPD (continuous Ambulatory Peritoneal Dialysis) with Dialysis Datalyser

To develop new products for kidney failure patients to help them decrease their suffering and enjoy their longer happy life. This contains dialysis treatment information in CAPD (continuous Ambulatory Peritoneal Dialysis) for patients with renal (kidney) failure.

Infection is a big risk. The patients will become ill if infection occurs in the peritoneum. The infection is called Peritonitis. Signs of infection are hazy or cloudy fluid. The patients may feel sick or vomit. The patients may have severe stomach pains. Early treatment will lessen the damage to the Peritoneum, lessen the risk of having to stay in hospital and will make the patients feel better more quickly.

Not draining enough fluid can be a problem. The patients could be in overload. Signs of being overload can check from the weight increase, feet/ankles swelling, shortness of breath, puffy eyelids, and raised blood pressure. Draining too much fluid can also be a problem. The patients could be dehydrated. Signs of dehydration are weight loss, you may feel dizzy or nauseous, suffer constipation or reduced blood pressure.

The Dialysis Datalyser can measure the total period of CAPD process, total draining fluid, the velocity of the fluid flow, early signs of infection, draining status at each stage of the CAPD process, status of dehydration and overload.

As an SME technology based startup with a higher degree in technology, it has tremendous strengths in addressing the market. In many cases the businesses are born in situations of a low degree of technology and product innovation processes readiness, including uncertain markets.

A technology uncertainly defines when development takes longer than expected, the technology does not act as intended or it is superseded by another. The innovation readiness levels and manufacturing readiness levels are used to confirm the level of technology certainly. Therefore, if the base technology is critically important to the product, then the technology uncertainly risk is the highest factor in their strategy.

Before the firm can engage in addressing a customer problem, it needs to be confident that they can develop the technology towards maturity and scale it economically. The concepts focus on the nature, technology and understand the technology to limit the risk. It also can choose to de-risk the technology if acceptable for the end product needs.

To de-risking technology or decreasing the amount of technology uncertainly can do with educating the customer to understand the degree of technology certainly. When technology uncertainly and market risk is high then patient resources are required.

An effective ecosystem to create patient resources funded from a large firm where the venture capital firm provides patient capital and change the technology technique to more sustained technology choices. Then, it moves from producing a product to a service based on core competency. The ecosystem was used for business development, grant development and early sales of the products to develop patient resources to underpin our technology and market.

Product innovators, start up or established devices suppliers, increasingly look for new materials and seek development manufacturing. The appetite for novel sensors, actuators and medical devices is challenging. There is an unprecedented rise in demand for data and sensing. The MEMS and micro systems market have a diverse range of applications [7]. The main mass commodity markets are automotive and consumer products.

With the new emerging model, grew out of provision of specialist manufacturing of high value, low volume products for the hospitals, academic and industry R&D sectors. It established as an independent commercial supplier of development and manufacturing services, bringing in new

management with backgrounds in electronic, smart materials and energy harvesting products and system. Considering the best way to create a functioning device means considering the process in order to minimize time and material spend, to reduce scrap, to improve yield and to minimize human error. Metrology, calibration and short loop design trials help ensure delivery against expectations during the development stage.

Support the patients' need, understand expectation and exceed them, appreciating the essential parameters and features of the medical devices. To apply creative can lead to a more efficient process and result in a fully functioning device with the greater commercial benefit. In innovation of specialist sensors, it needs open communication and flexibility ability to scale.

Production capability is experiencing a combine tool set, know-how and innovation. The ISO9001 is a useful stamp of quality [8]. The value-add of an experienced and creative team with its ability to steer a design into volume production. It needs to understand specification, optimization, testing, metrology, design for manufacturability and system integration. It must have links to supply chain partners and optimise production.

IV. CONCLUSIONS

Electrical circuit elements were used to simulate the properties of blood vessels in the kidney. The renal blood vessels impedance can provide more information on the physical properties of the renal system. The parameters of the renal blood vessels show the resistance is greatest at a section of the segmental artery.

This indicates that the blood flow starts to reduce the speed and the blood pressure drop occurs in the smaller artery. The large capacitance could indicate higher elasticity. Therefore, the arcuate artery could have a higher elasticity than the others.

To develop new products for kidney failure patients to help them decrease their suffering and enjoy their longer happy life, infection is a high risk. Early treatment will lessen the damage both physical and financial terms. The innovation readiness levels and manufacturing readiness levels are critically important to the product. In addition, the technology uncertainly risk is the highest factor.

This study presents results which, it is hoped, will lead to further development in non-invasive renal medical devices for use in the treatment of blocked renal vessels in chronic kidney failure.

ACKNOWLEDGMENT

The authors would like to acknowledge the financial support from the Ronsek Limited, UK for the supply of components and I would like to special thanks to Dr Paul Weaver for knowledge contribution.

REFERENCES

- [1] K. Pechrach, "Modeling of Renal Vascular System for Nanomedical Applications", Franco-British Nanomedicine Summit Countdown to FP7, Paris, France, November 2006.
- [2] Hill A, Surat R, Cobbold R, Langille L, Mo L, Adamson L, "A wave transmission model of umbilicoplacental circulation based on hemodynamic measurement in sheep", *Am. J. Physiol*, 206, 1267-1278.
- [3] www.mc.edu, www.bio.psu.edu, www.nursingcenter.com
- [4] Milnor R, "Vascular impedance Hemodynamics", 1989, 167-203.
- [5] Guyton C, "Formation of urin by the kidney: renal blood flow, glomerular and their control", *Medical Physiology*, 1991, 286-297.
- [6] Hsu L, Hsiu H, Chao P, Li S, Wang W, Wang Y, "Three-block electrical model of renal impedance", *J. Physiol Meas* 26, 2005, 387-399.
- [7] MacBeth and B. Dunne, "Mind the Gap!", *CMM International Commercial Micro Manufacturing*, Volume 9, No 6.
- [8] R. Giasolli, R. Kolkman, Y. Marinakis, S. Walsh, "Emerging Additive Manufacturing and Nanotechnology Can Embrace Lean Startup Techniques", Volume 9, No 6.



Dr. Kesorn Pechrach Weaver is a R&D Director in Ronsek Ltd. She is a specialist in Electro-Mechanical Engineering and research scientist. She graduated PhD. from University of Southampton, UK and Master degree in Energy Engineering from King Mongkut's University of Technology Thonburi, Thailand and Bachelor degree in Electrical Engineering from Khon Kaen University. Her expertise includes medical devices, arc imaging, circuit breakers, smart material piezoelectric, medical devices and energy harvesting. In addition, she is an electrical engineer covering design and site construction supervision in oil refinery plants, substations and industrial estate She is a Chartered Electrical Engineer of the Engineering Institute of Thailand and a member of the IEE.

Fault Characteristics of PV Power Plant Grid Integration by PSCAD/EMTDC

Nattapan Thanomsat

Department of Electrical Engineering, Faculty of
Engineering
Rajamangala University of Technology Thanyaburi
Pathumthani, Thailand
nattapan@mail.rmutt.ac.th

Boonyang Plangklang

Department of Electrical Engineering, Faculty of
Engineering
Rajamangala University of Technology Thanyaburi
Pathumthani, Thailand
boonyang.p@en.rmutt.ac.th

Abstract— Thailand Ministry of Energy has estimated that Photovoltaic Power Plant (PV Power Plant) will be occupied 22% in 2021 of the renewable energy sources. From current reports, when a large scale Photovoltaic Power Plant is connected to the grid distribution system, protective devices will be working improperly and therefore occurred problems due to the integration of PV Power Plant. For example, the current of integrated PV Power Plant would cause Wye-grounded/Delta winding of interconnection distribution transformer in saturation characteristic and there are many reasons to cause the grid system failed. This paper will model difference condition faults by PSCAD/EMTDC. The simulation result shows that the fault current contribution from PV system depends on a number of different factors, not only on the size of the PV system.

Keywords— Photovoltaic power plant, Grid distribution System, faults analysis

I. INTRODUCTION

Nowadays, the international community realizes serious global warming with increasing the pollution from using fossil fuel. A lot of countries, including Thailand, have used renewable energy. The most of them is the increasing of used PV for generated electric and this tendency is expected to continue in the next year [1]. The renewable energy with Alternative Energy Development Plan 2015 (AEDP 2015) has supported by the Thai's government, which point to increase the using renewable energy in generated electricity, preferably photovoltaic system, to 6000 MW by the year 2036 [1].

The transmission, distribution of the electric energy produced in parallel with the efforts to raise the generated electricity and the management of the malfunctions that may occur in the system are required to be managed. The goal of the electricity authority that produces, proceeds and distributes electricity is to supply continuous, affordable and good quality service to their end-users. The failures in distribution lines happen as a result of short circuits in generator, transformer, and reparative switchgear or due to isolation. Detection of these failures, their start and finish time are of utmost importance for problem-solving [2], [3], [4].

However, if the large capacity installed PV systems are connected to grid, a few problems can be happened. For

example, if an accident occurs single line to ground fault at distribution line with PV system, fault current is fluctuate being up to the install capacity of PV system and transformer. So it can create protective element cause the crash problems. For this reason, it is very important and essential to consider trouble between distribution network and PV system.

Under these condition, this paper analyze three-phase fault, by using PSCAD/EMTDC modeling analysis [5], [6], and [7].

II. MODELING FOR PV SYSTEM AND DISTRIBUTION SYSTEM

Table 1 shows the specification of network components and the specification for power distribution at loads. With this data, the modeling system was operated by using PSCAD/EMTDC [8] as shown in Fig 1.

A typical power distribution network for providing power to the loads has been considered as a test network for the analysis. The test model of the network is shown in Fig. 1. Three phase power at 22 kV is supplied via overhead line (OHL) from main substation to pole mounted 22/0.4 kV. The incoming power from the PV source is protected and switched by PV system's integral switching and protection device. Specifications of the components for the network in Fig. 1 are provided in Table 1 in Appendix. For the purpose of this study, two loads have been considered. Considering a maximum demand of 500 kVA per load A roof top photovoltaic system of 500 kW for each load has been considered.

TABLE I: The specification of network components and the specification for power distribution at loads

Description	Specification
Utility Supply Voltage	22 kV, 3 phase, 50 Hz
Transformer	22/0.4 kV, 1 MVA, 3 phase, 50 Hz, Delta/Wye-ground
Load	500 kVA per Load
PV system	500 kW per PV system

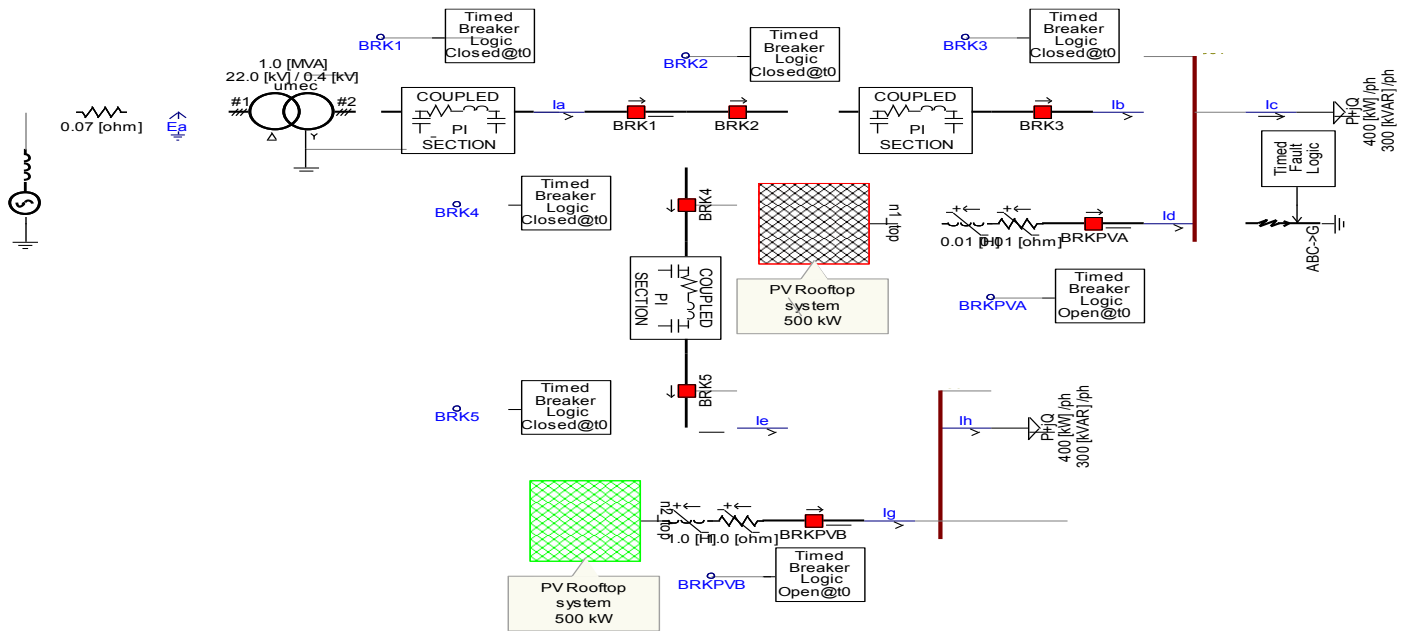


Fig. 1. The test model network by using PSCAD

III. CASE STUDIES AND SIMULATION

Four different cases have been analyzed during a fault in the Load 1. The cases have been described in this Sections A-D:

A. *Fault at the Bus 01 of Load 1 when only utility power source is connected to Load 1 (PV system is not connected)-Case 1*

This case represents the flow path for fault current during a three phase fault in the Bus01 of load 1 when PV system is not connected to grid. The fault current flowing through BRK2 and BRK3 is 0.7 kA. The simulation output for the fault is shown in Fig. 2. A three phase to earth fault was applied at 0.2 s for duration of 0.1 s.

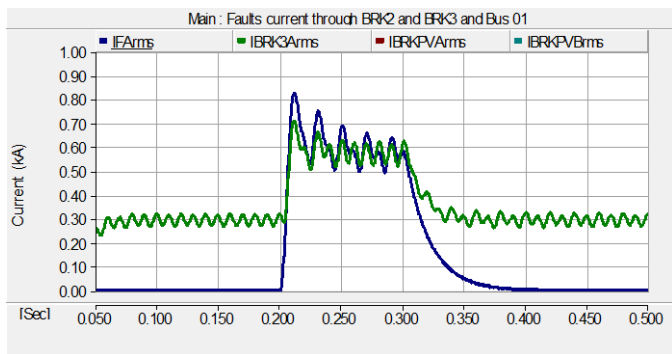


Fig.2. RMS value of fault current for case 1.

B. *Fault at the Bus 01 of Load 1 when utility power source is available and PV system (PVA) is connected to Load 1 only.Case 2*

This case represents the flow path for fault current during a three phase fault in the Bus 01 when PV system is connected to the Load 1. The simulation output for the fault is shown in Fig. 3.

A three phase to earth fault at Bus 01 was simulated at 0.2 seconds for duration of 0.1 seconds. In this case additional fault current is contributed by PVA. Though this additional fault current has increased the value of total current at the point of fault from 0.8 kA to 0.9 kA, the fault current flowing through circuit breaker BRK2 and BRK3 is still the same (i.e. 0.7 kA) as case 1. The additional fault current contribution from PVA therefore does not disturb the protection coordination of the network as the additional of current does not flow through BRK2 and BRK 3.

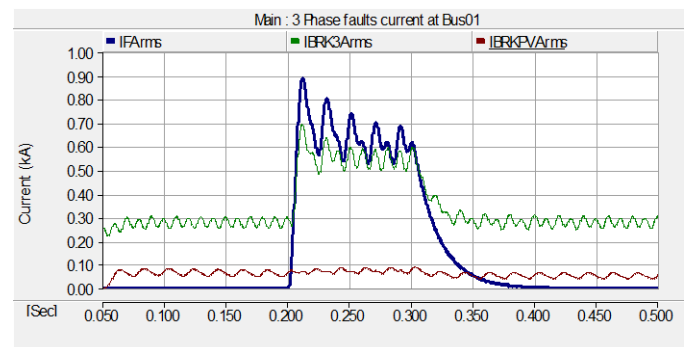


Fig.3. RMS value of fault current for case 2.

C. Fault at the Bus 01 when utility power source is available and PV systems PV-A is connected to Load 1 and PV-B is connected to Load 2-Case 3

This case represents the flow path for fault current during a three phase fault in the Bus 01 when a PV system is connected to the Load 1 and 2. The simulation output for the fault is shown in Fig. 4. In this case, there will be an additional fault current contribution from PVA and from PV-B. The value of total current at the point of fault will increase from 0.9 kA (in case 2) to 0.92 kA. The fault current flowing through circuit breaker BRK2 and BRK3 in this case will increase from 0.7 kA to 0.71 kA due to contribution of fault current from PV-B.

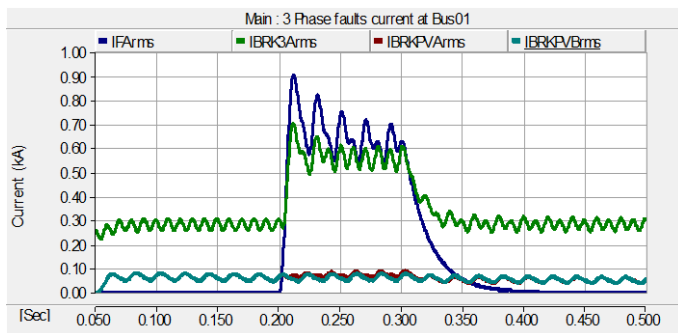


Fig. 4. RMS value of fault current for case 2

D. Analysis for switching one circuit breaker operated on transformer

In the circumstance of the malfunction in the power system, with connecting and dis-connecting circuit breakers and ground fault missing that can be occurred Ferroresonance, because a nonlinear saturated iron core inductor of transformer is substituted into the LC circuit.

Ferroresonance is nonlinear resonance phenomenon that can affect power networks. The problem with this phenomenon is an over voltage and over current.

In this paper, after single line to ground fault happened, the iron core inductor of transformer was saturation. The switching circuit breakers was operated single phase and re-close and close on 0.325 s. and 0.525 s. The simulation results for Ferroresonance phenomenon is obtained as shown in Fig. 5.

Ferroresonance can generate over voltage more than 80 kV. That mean, if this phenomenon stays long time, transformer could be defect and other electrical equipment is affected.

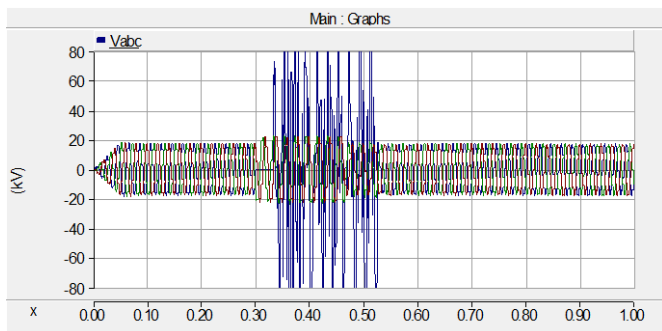


Fig. 5 Simulation of Ferroresonance

IV. CONCLUSION

This paper has been interested for the analysis of fault in the distribution network with PV system, and proposed the comparison of malfunction analysis by using the simulation software PSCAD/EMTDC. The results are concluded hereinafter; four cases have been considered in Section 3. The first case study does not consider any fault current contribution from the PV system and cases 2, 3 and 4 represent scenarios for studying effects of incremental fault current contribution from PV systems on protection system. It is observed from the case 2 that the contribution of fault current from the PV system connected to a Bus where fault has occurred does not have any impact on the protection system of the overall system. It is only the fault current from the PV systems connected to Bus of other Loads (where no fault has occurred) that has the potential to disturb the existing protection coordination of the protective devices supplying power to the Bus where the fault has occurred. As observed in case 3, it is also important to note that, while the PV system connected to the Bus where fault has occurred will contribute the full (expected) magnitude of fault current to the point of fault, the fault current contribution from a PV connected to the Bus of other Loads will be less than 100 A. The available additional fault current flowing through BRK2 and BRK3 is not a direct multiple of the possible fault contribution from an individual PV but depends on a number of other factors including, the loading of the buses and the cable length between the Bus and the low voltage distribution. As observed in case 4, it is also confirmed that if transformer is saturation and switching breaker single phase is operated, Ferroresonance could be occurred and make all electric device defected. Therefore, when the PV power plant installed, the protective devices have to be considered and adjusted.

REFERENCES

- [1] N.Chimres and S.Wongwises, "Critical review of the current status of solar energy in Thailand" Renewable and Sustainable Energy Review, vol.58, pp 198-207, 2016.
- [2] T.C. Akinci (2009). Determination of ferroresonance phenomenon with spectral and wavelet analysis methods in power systems", Ph.D. Thesis, Marmara University, Institute of Pure and Applied Sciences, Istanbul, Turkey. (In Turkish).
- [3] T.C. Akinci (2005). Wavelet based distributing systems of protection algorithm", Master Thesis, Marmara University, Institute of Pure and Applied Sciences, Istanbul, Turkey. (In Turkish).
- [4] A.J. Pansini (1990). Basics of Electrical Power Transmission, Prentice Hall, ISBN: 013-059866-6, New Jersey, USA, pp.1-13.
- [5] Son, J., Kim, B., Rho, D.: "A Study on the Optimal Operation Method for Protective Devices at the Primary Feeders Inter connected with New Energy Sources." In: IASTED Conferences, pp. 696-701 (2010)
- [6] Barker, P.P., de Mello, R.W.: "Determining the impact of distributed generation on power systems: Part 1 - Radial distribution systems." In: Proc. IEEE Power Eng. Soc. Summer Meeting, vol. 3, pp. 1645-1656 (2000)
- [7] Arritt, R.F., Dugan, R.C.: "Distributed generation interconnection transformer and grounding selection." In: Power and Energy Society General Meeting - Conversion and Delivery of Electrical Energy in the 21st Century, pp. 1-7. IEEE (2008)
- [8] N.Thanomsat and B.Planklang, "Modelling of a Micro Grid PV Rooftop System by PSCAD" International Conference on Energy: World Future Alternatives (NU-ICE 2015)

A Methodology for Forecasting Electrical Energy Demand

N. Phuangpornpitak

Faculty of Science and Engineering, Kasetsart University
Chalermphrakiat Sakonnakhon Province Campus
Sakonnakhon 47000 Thailand
E-mail: napaporn.ph@ku.ac.th

B. Prasartkaew

Faculty of Engineering
Rajamangala University of Technology Thanyaburi
Thanyaburi, Pathumthani 12110 Thailand
E-mail: boonrit.p@en.rmutt.ac.th

Abstract — Forecasting electricity in the future is an important information resource in planning and distribution in electric systems. This paper aims to study electricity demand forecasting of Sakonnakhon province. Electrical energy demand could be forecasted by using the mathematical model. The statistical data of electricity demand in the past, and meteorological data are input variables used in the model. The electrical users can be classified into four categories as (i) home and residential users, (ii) small business, (iii) medium and large businesses and (iv) other applications such as pumping water system for agricultural purpose. The proposed models are validated by using the previous data of electrical usage and meteorological data in 2012-2014 to predict the electrical demand usage in 2015. The proposed model has an error of 4.61%. The experimental results show that the forecasting electricity demand of Sakonnakhon province in 2016-2018 are found to be 701,876,573 kWh, 770,268,919 kWh and 838,244,233 kWh, respectively.

Keywords — *Electricity demand forecasting; Energy model; Power system management; Load forecasting; Renewable energy; Sustainable development*

I. INTRODUCTION

Due to the fast growing economy and population in developing countries, energy is one of the key factors to support economic growth and meet the ongoing energy demand. Energy sector is playing a significant role in Thailand economy by running the wheel of industries and transports. In terms of energy demand by sector, the transport sector dominated the energy use with 36% share, followed by industrial sector as 35%, residential and commercial as 23%, agricultural sector as 5% and non-energy use as 1% [1]. Forecasting electricity consumption in the future has become a major task of an electricity organization which involved in the supply of electricity to meet the demand. During the last decade, electricity consumption and peak power demand in Thailand trend to increase continuously. The use of electricity and peak power demand in Thailand shows the variation in behavior and relationship between electricity consumption and economic growth of the country.

Electricity demand forecasting is an essential process in electric power system operation and planning. It involves the accurate prediction of both magnitudes and geographical locations of electric load over the different periods of the planning horizon. Many economic implications of power utility such as economic scheduling of generating capacity, scheduling of fuel purchases, security analysis, planning of power development, maintenance scheduling and dispatching of generation units are mainly operated based on accurate load forecasting.

Load forecasting can be divided into three categories: short-term forecasts, medium-term forecasts and long term forecasts. The natures of these forecasts are different as well. Short-term forecasts are usually from one hour to one week. They play an important role in the day-to-day operations of a utility such as unit commitment, economic dispatch and load management. A short term electricity demand forecast is commonly referred to as an hourly load forecast. Medium-term forecasts are usually from a few weeks to a few months and even up to a few years. They are necessary in planning fuel procurement, scheduling unit maintenance, energy trading and revenue assessment for the utilities. A medium-term forecast is commonly referred to as the monthly load forecast. Long-term electricity demand forecasting plays an important role in the electric power system planning, tariff regulation and energy trading [2]. A long-term forecast is required to be valid from 5 to 25 years. This type of forecast is used to deciding on the system generation and transmission expansion plans. A long term forecast is generally known as an annual peak load.

This paper aims to address the electricity demand forecasting. The develop model has been used as a tool to predict the future demand. In order to make a distribution in the assistance for decision maker this study attempts to identify and analyze the load demand forecasting in Sakonnakhon province which located in the northeastern region of Thailand. The forecasting accuracy and precision would be useful for planning and strategy in the electricity generation and supply of energy resources.

II. PRINCIPLE

The objective of short-term load forecasting is to predict the near future load for example load prediction or next day load prediction. The total system load is the load seen at the generating end of the power system, which includes the sum of all types of loads connected to the system plus the losses. There are several factors which influence the behavior of the consumer load and also impact the total losses in transmission lines. These factors are time factor, weather, economy, possible customers' classes and random disturbances.

The medium- and long-term forecasts take into account the historical load and weather, the number of customers in different categories, the appliances in the area and their characteristics including age, the economic and demographic data and their forecasts, the appliance sales data, and other factors. The time factors include the time of the year, the day of the week, and the hour of the day. There are important differences in load between weekdays and weekends. The load on different weekdays also can behave differently. Electricity demand of a power system is mainly influenced by time factor, economic factor, weather condition and customer type.

A. Time Factor

Time is the most important factor in load forecasting since its impact on consumer load is highest. Fahad and Arbab (2014) note that the observing load curve of different grid stations is periodic [3]. In addition, load demand reflects the consumer's daily lifestyle. The study indicates that the maximum demand occurs at 8 pm, and minimum load demand occurs after midnight. At midnight everyone is sleeping so there is no need of lighting, heating or cooling the home, thus load becomes least. Similarly at about 8 pm everyone is at home doing activities together, thus load is highest at that part of the day.

The daily activities of people can be classified into three parts:

- Working time
- Leisure time
- Sleeping time

It is noticed from the collected load data that the load curve is periodic. The periodic of load curve occurs not only in the daily load, but also in the weekly, monthly, seasonal and yearly load curves. By taking the periodic property, load forecast can be predicted effectively.

B. Economic Factor

Economic factor has an impact on the usage of electricity. The average consumption per unit consumer depends on the economic factor including the following

- Gross Domestic Product (GDP)
- Average household income
- Income distribution

These factors reflect the economic situation of the country. Electricity price and the people's buying capability also have impact on the usage of electricity. The more expensive the electricity is, the less use of electricity by the domestic consumers. Time of use pricing can change the duration and the time of occurrence of peak load. Time of use pricing can also make domestic as well as industrial consumers to adjust their load and thus helps in peak shaving.

C. Weather Condition

Weather conditions influence the load. In fact, forecasted weather parameters are the most important factors in load forecasts. Various weather variables could be considered for load forecasting.

- Temperature
- Humidity
- Precipitation
- Wind speed and wind chill index
- Cloud cover and light intensity

Temperature and humidity are the most commonly used load predictors to minimize the operational cost.

D. Customer Type

Most electric utilities serve customers of different types as following:

- Residential consumer
- Commercial consumer
- Industrial consumer

The electric usage pattern is different for customers that belong to different classes but is somewhat alike for customers within each class. Therefore, most utilities distinguish load behavior on a class-by-class basis.

III. APPLICATION OF THE MODEL

The model aims to predict the electricity demand by using the previous data of electrical usage and meteorological data. The method was applied to Sakonnakhon province. The reasons for selecting this area for applying the model because of the availability of data (i.e. the meteorological data and the electricity usage of study area). Fig.1 shows the location of the study area. Sakonnakhon province located in the Northeast of Thailand which the total area of 9,605.8 km². The latitude of the area is 17.09°N and longitude is 104.08°E. The average temperature of the area ranges from 14-34°C.

A. Data Collection

The data used in the present case study are:

- Data of electricity consumption and population
- Meteorological data of the province

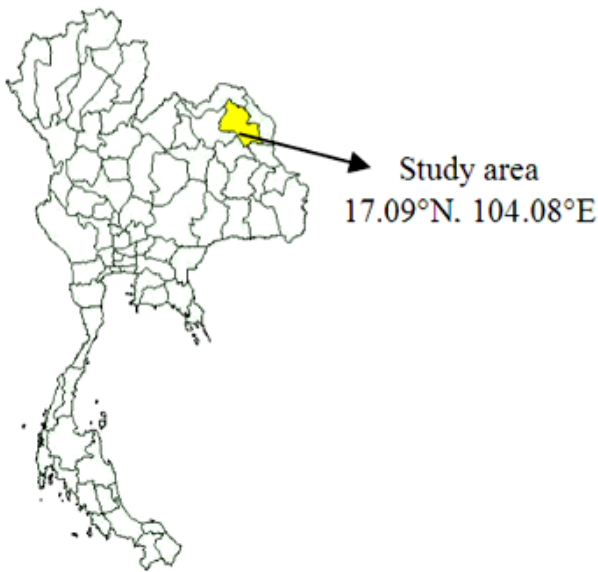


Fig. 1. Location of the study area

Fig. 2 shows the topographic map of Sakonnakhon province. The map shows the administrative boundary, river network, road network and settlement of the study area. There are 18 districts in Sakonnakhon province. Fig. 3 shows the population density of the study area. At present, the total population of Sakonnakhon province is 1,140,229¹.

Administrative map of Sakonnakhon

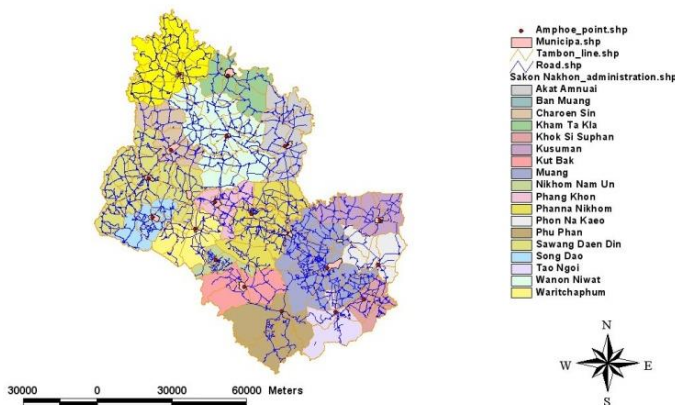


Fig. 2. Topographic map of Sakonnakhon province, Thailand

Population density

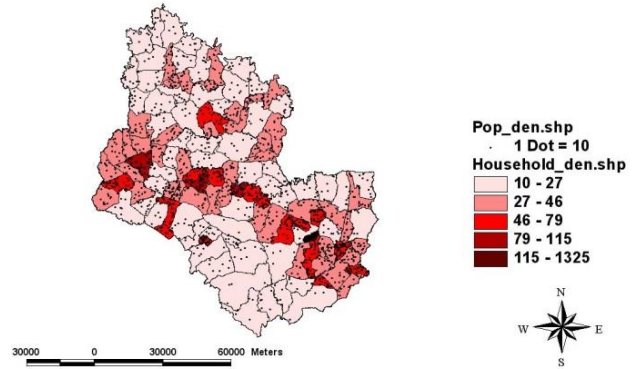


Fig. 3. Population density of the study area

B. Load Demand

The electricity demand in each commune of Sakonnakhon province is built up from two sectors: household and non-household. The electricity consumption of commercial (small industry, handicraft and service), and public sector is categorized as non-household energy consumption (hospitals, schools, street lighting, etc.). In this study, not only institution and small industry loads were considered, but also other big loads and the point loads like agricultural loads were considered.

An innovative map of electricity demand of Sakonnakhon province was studied by Phuangpornpitak [4] which the electricity demand scenario of the location can easily be understood. Fig. 4 shows the electricity demand map of Sakonnakhon province. The maximum demand of electricity lies between 29.3-60.9 GWh/year and the minimum energy demand is within 0-2.3 GWh/year as shown in the figure.

Energy demand

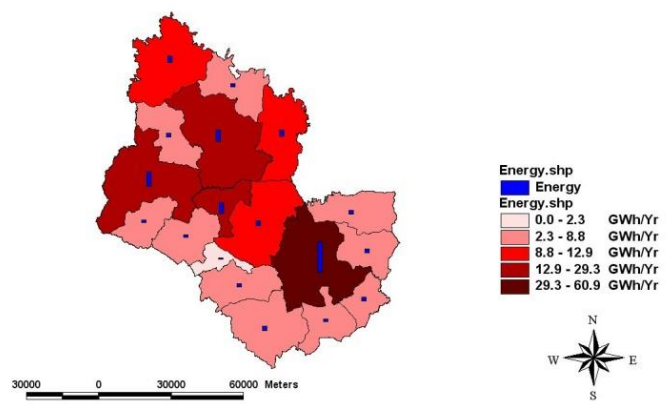


Fig. 4. Energy demand of the study area

¹ Data obtained from National Statistical Office (December 2015)

C. Forecasting Technique

Electricity demand forecasting techniques can be classified as follows:

- Multiple regression
- Exponential smoothing
- Iterative reweighted least-squares
- Adaptive load forecasting
- Stochastic time series
- Neural networks

The problem formulations of these techniques are discussed by Almeshaii and Soltan [5] and Soliman and Ahmad [6]. The regression model of weighted least-squares estimation has been used in this study. Based on this analysis, the statistical relationship between total load and weather conditions as well as the day type influences can be calculated by using equation (1). The regression coefficients are computed by a weighted least square estimation using the defined amount of historical data [7].

$$Y_t = v_t a_t + \varepsilon_t \tag{1}$$

where,

- Y_t : Measured system total load,
- v_t : Vector of adapted variables such as time, temperature, light intensity, wind speed, humidity and day type (workday or weekend),
- a_t : Transposed vector of regression coefficients,
- ε_t : Model error at time t , and
- t : Sampling time.

IV. RESULTS AND DISCUSSION

This study carried out the model studies and survey on the electrical energy demand of Sakonnakhon province which located at the northeastern part of Thailand. Observation and analysis of results have been used to validate the model proposed. The electrical users can be classified into four categories as:

- (i) Home and residential users
- (ii) Small business
- (iii) Medium and large businesses
- (iv) Other applications such as pumping water system for agricultural purpose

Fig. 5 shows the forecast results compared with the actual electrical energy demand for each electrical user type to investigate the error of models in each category. The predictive electricity demand for residential users has the minimum error of 2.16% compared with other user types. The model has the maximum error of 32.07% for other electrical users, i.e. agricultural purposes. The application of this model has an error of 8.82% for small business and 12.44% for medium and large businesses.

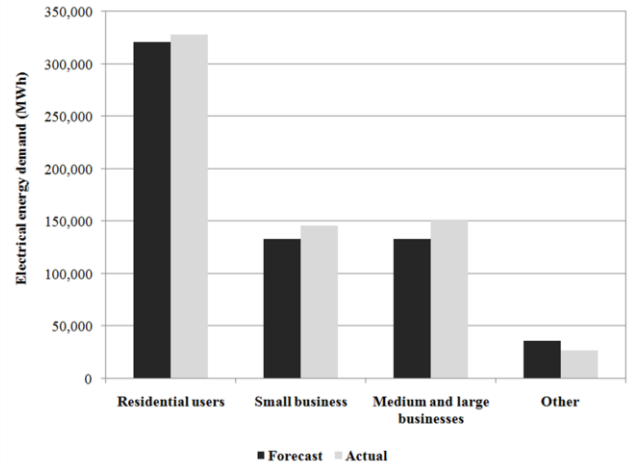


Fig. 5. Comparison the forecast results with the actual demand by user type

Fig. 6 shows the forecast results from the model with the actual electrical energy demand in 2015. The predictive electricity demand of the province in 2015 was 622,805,767 kWh, while the actual electricity demand was 652,924,018 kWh. Thus, the proposed model has an average error of 4.61%. January has the minimum error as 0.40%, while July has the maximum error as 8.61%.

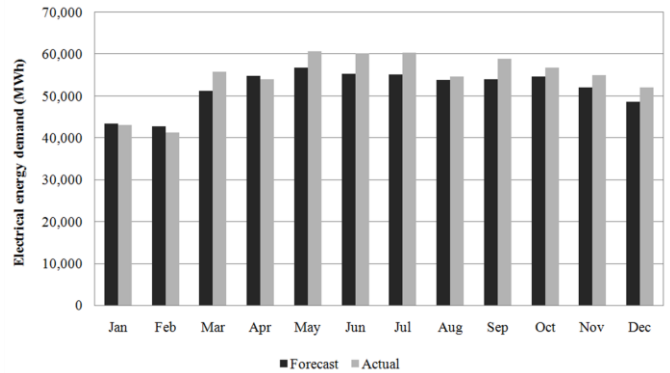


Fig. 6. Comparison the forecast results with the actual demand

Table I presents the increasing rate of electricity demand annually. The increasing rate of electricity demand in 2013-2015 has an average of 5.86%. The increasing rate of electricity demand in the past year was the lowest in 2013 which equals to 4.64% and the increasing rate of electricity demand is highest in last year (2015) which equals to 7.33%. The forecast results obtained from the model indicate that the increasing rate of electricity demand for the next three years (2016-2018) has an average of 8.69%. The increasing rate of electricity demand is mainly due to the province plan to invest trade for supporting ASEAN economic community and increasing number of population.

TABLE I. INCREASING RATE OF ELECTRICITY DEMAND ANNUALLY

Year	Electrical energy demand increase from last year (kWh)	Increasing rate (%)
2013	575,941	4.64
2014	608,358	5.63
2015	652,924	7.33
Average in the past 3 years		5.86
2016	701,877	7.50
2017	770,269	9.74
2018	838,244	8.82
Average 3-year forecast		8.69

V. CONCLUSION

The model has been developed in this study to predict the electrical energy demand. It introduces an integrated approach which estimated the electricity demand of the selected area. This methodology can be applied in any location to predict electricity demand of that location thus help the policy makers to plan for energy supply project implementation. The load forecasting model in this study takes into account the local constraint and conditions such as the previous electricity consumption of the region under consideration, the number of population and households and the meteorological data. The process of predicting electricity demand adapted in this study using technical analysis can serve as an example to evaluate the load demand forecast of Sakonnakhon province. The model has been validated by using electricity demand of the year 2015 and thus predicts the electricity demand of Sakonnakhon in 2016-2018. This method can be further extended to conduct a comprehensive study for national level in order to grasp the load demand of the country.

Acknowledgment

The authors are grateful to the Thailand Research Fund (TRF), the Faculty of Science and Engineering, Kasetsart University, Chalermphrakiat Sakonnakhon Province Campus, the Kasetsart University Research and Development Institute (KURDI), and the Research and Development Institute of Chalermphrakiat Sakonnakhon Province Campus for the scholarship support in conducting this study.

REFERENCES

- [1] EPPD, *Thailand Energy Report 2015*. Energy Policy and Planning Office, Ministry of Energy, Thailand, 2016.
- [2] J. F. M. Pessanha and N. Leon, "Forecasting Long-term Electricity Demand in the Residential Sector," *Procedia Computer Science*, vol. 55, pp. 529-538, 2015.
- [3] M. U. Fahad and N. Arbab, "Factor Affecting Short Term Load Forecasting," *Journal of Clean Energy Technologies*, vol. 2, pp. 305-309, 2014.
- [4] N. Phuangpornpitak, "Evaluation of Solar Energy Potential for Electricity Generation Using Geographic Information System," *GMSARN International Journal*, vol. 4, pp. 23-30, 2010.

- [5] E. Almeshaiei and H. Soltan, "A methodology for Electric Power Load Forecasting," *Alexandria Engineering Journal*, vol. 50, pp. 137-144, 2011.
- [6] S. A. Soliman and M. A. Ahmad, *Electrical Load Forecasting: Modeling and Model Construction*: Elsevier, 2010.
- [7] H. K. Alfares and M. Nazeeruddin, "Electric load forecasting: literature survey and classification of methods," *International Journal of System Science*, vol. 33, pp. 23-34, 2002.

IEET Editorial Office

EAAAT - Electrical Engineering Academic Association (Thailand)
Room 409, F-Building
140 Cheum-Sampan Rd.
Nong Chok, Bangkok, Thailand 10530
Tel: +662-988-3655 ext 2216 Fax: +662-988-4026

www.journal.eeaat.or.th

